068670-11-P COO-1407-49

College of Engineering
Department of Atmospheric and Oceanic Science

Progress Report No. 9

RAIN SCAVENGING STUDIES

A. Nelson Dingle

U.S. Atomic Energy Commission
Contract No. AT(11-1)-1407
Argonne, Illinois

July 1973

TABLE OF CONTENTS

LIST OF TABLES AND FIGURES

SECTION I: RESEARCH IN PROGRESS

A. Temporal and Spacial Resolution of Data for Tracer Experiment of 1 June 1970

Abstract

Further detailed study of precipitation patterns from the ISWS raingauge network and synoptic weather data for the 1 June 1970 experiment requires modification of previous interpretations based upon tracer deposition and radar echo propagation. Shortcomings of the previous studies relate mainly to the radar data which now are shown to have been more attenuated than previously expected. Frontal activity at and near the level of emission of tracer, and a cyclonic center south of the research area, when carefully analyzed lead to more complete insight into the westward transport of tracer material and help to explain an extended delay of tracer deposition at some of the sequential sampling stations. Implications for silver iodide cloud modification by vaporized releases in the vicinity of a frontal surface are derived from the observed patterns of tracer deposition.

1. INTRODUCTION

The present study represents a further analysis of the data initially discussed in Dingle (1972), referred to below as (D). Essentially, we have four independent sources of information about the motion field and its behavior under the influence of the synoptic weather systems of 1 June 1970. The first is the synoptic weather data including the 1900 CDT rawinsondes, the second is the ISWS radar data, third is the ISWS rain gauge network data, and fourth is the evidence of tracer indium in sequential samples taken at six stations (G•1, G•2, G•3, $\dot{M}$, M•1 and M•2). To the extent that these information sources yield conflicting evidences, a distortion of the wind field by the convective activity is indicated, and the time scale of the tracer trajectories into and out of the rain-generating processes is implied. These therefore supply a kind of definition to the problem that places restrictions upon a proposed model.

2. SYNOPTIC WIND FIELD

The general synoptic situation at 0700 CDT on 1 June 1970 is shown by the surface and 500 mb weather maps (Fig. 1 and 2). More specific surface data are provided by the 1600, 1700, 1800 and 1900 CDT sectional maps (Fig. 3 thru 6). These support the inference that the 1900 CDT sounding at

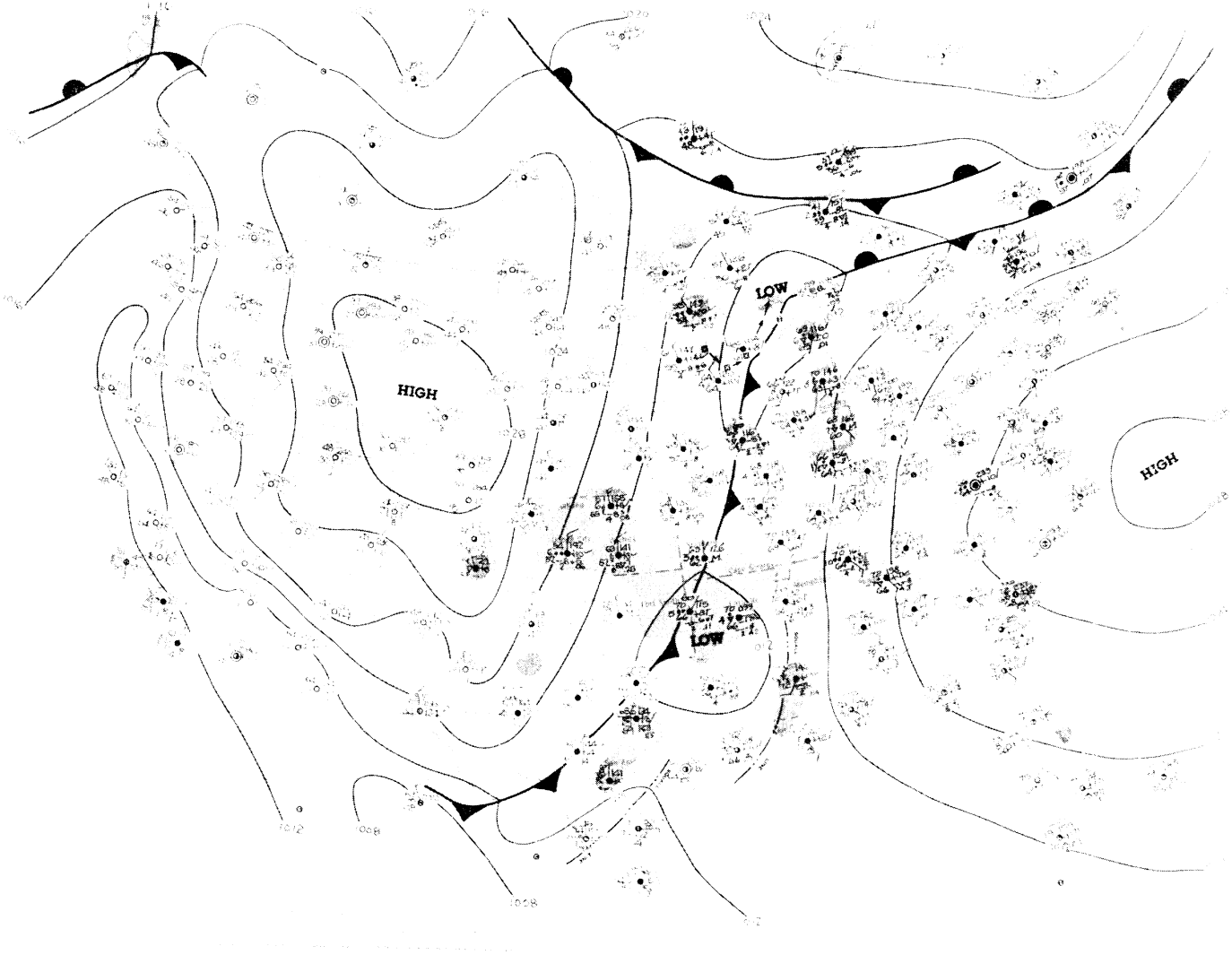

Fig. 1. Sea level weather map, 0700 CDT, 1 June 1970

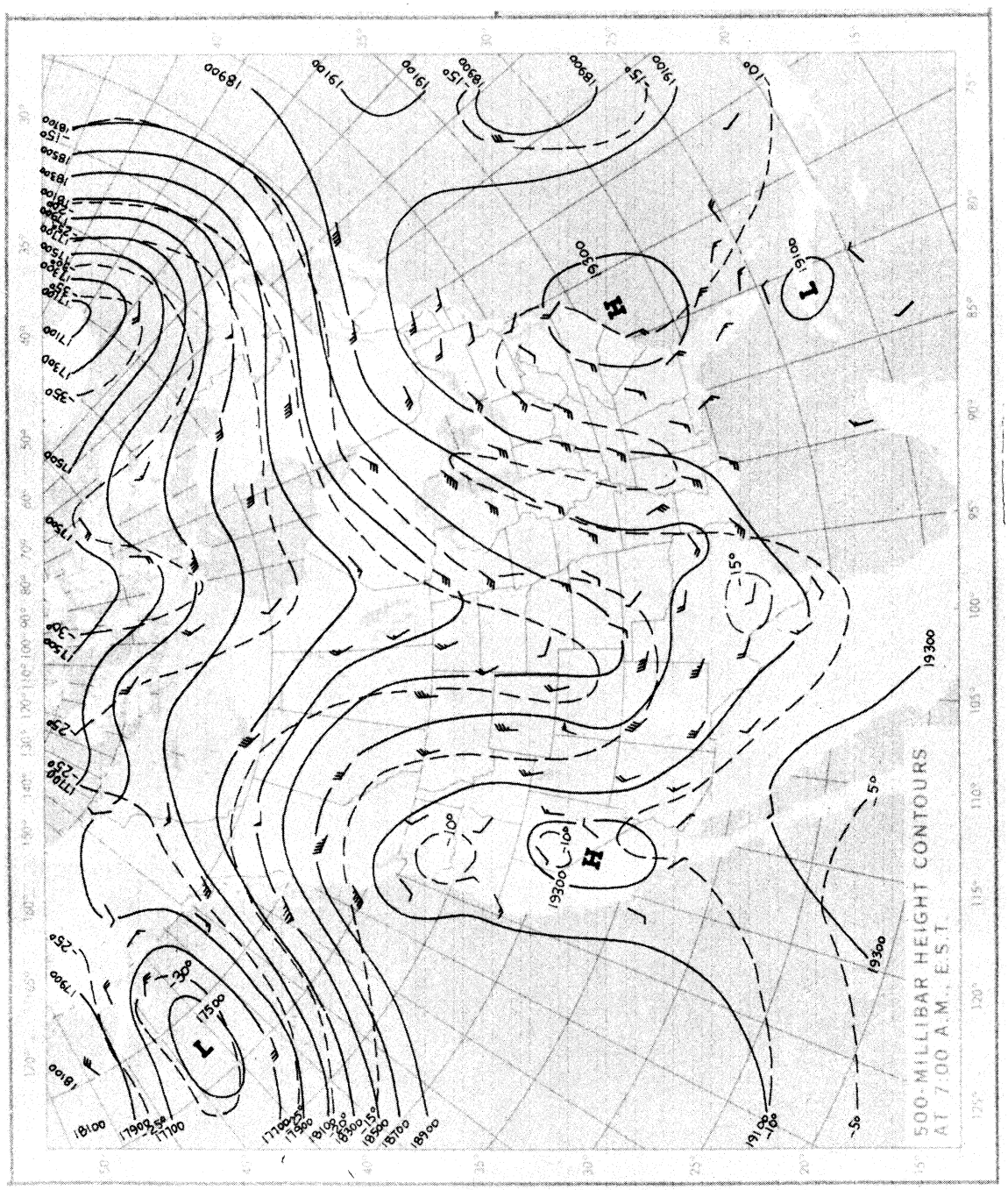

Fig. 2. 500 mb level weather map, 0700 CDT, 1 June 1970

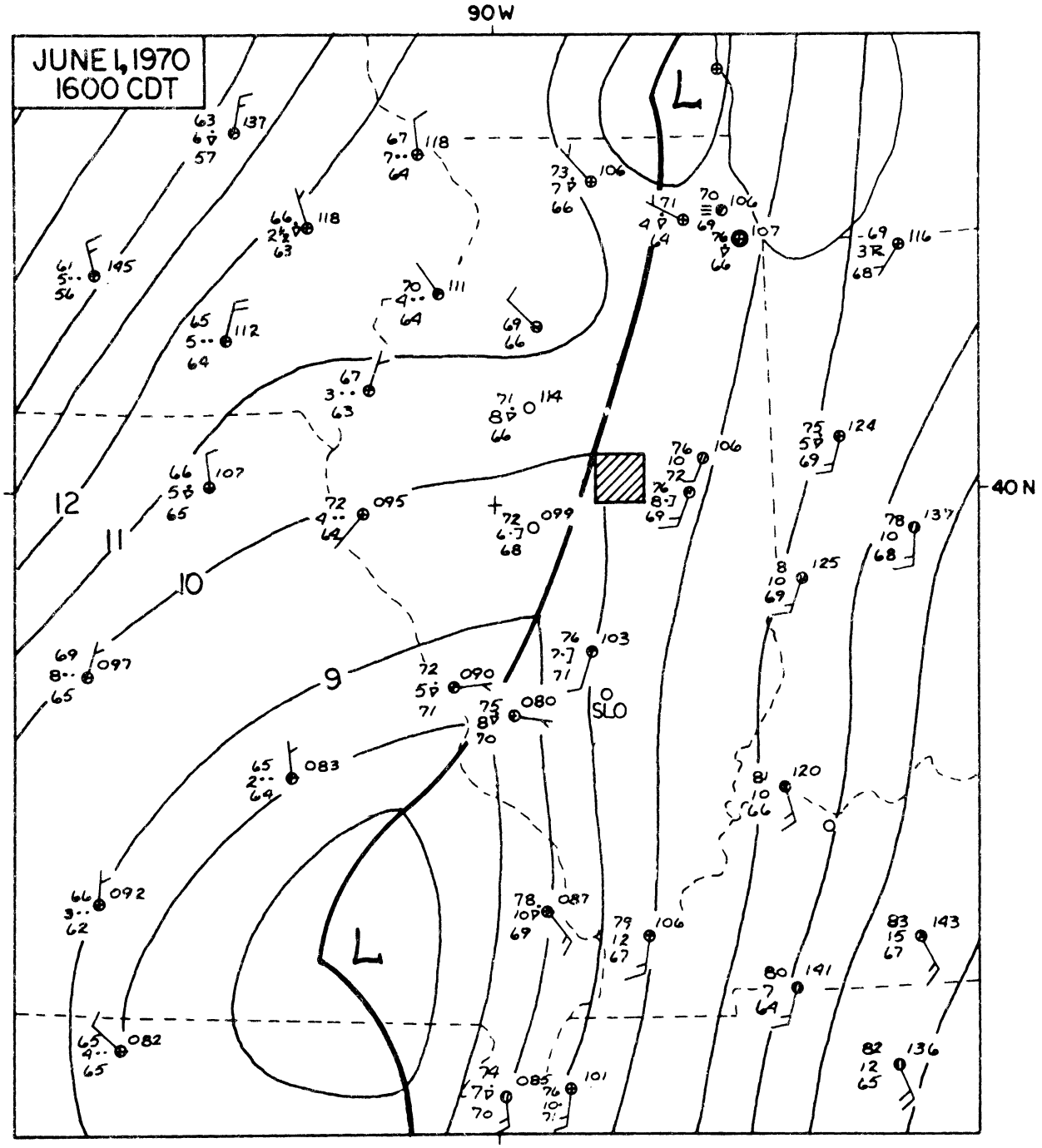

Fig. 3. Sea level sectional weather map, 1600 CDT, 1 June 1970

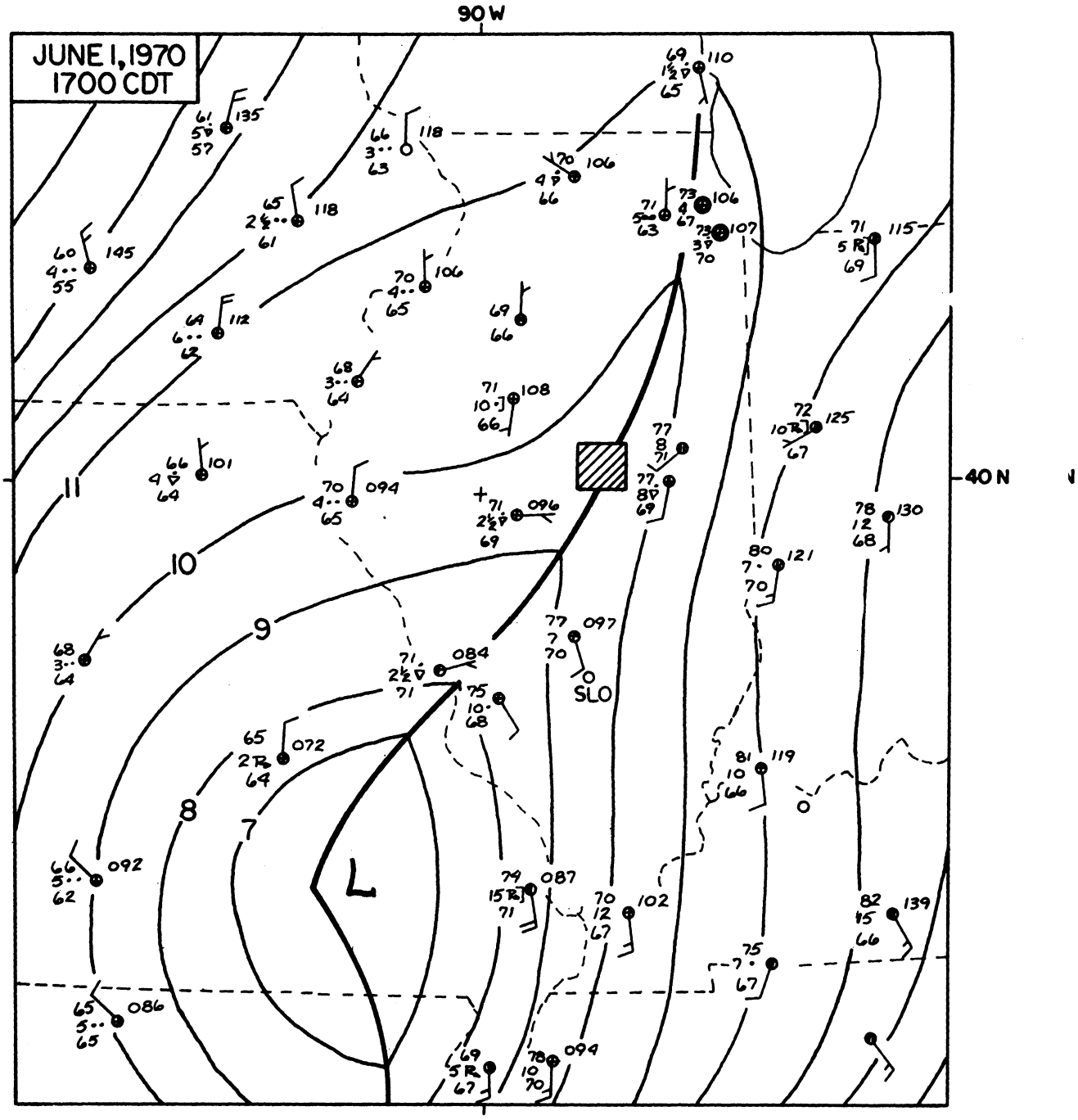

Fig. 4. Sea level sectional weather map, 1700 CDT, 1 June 1970

7

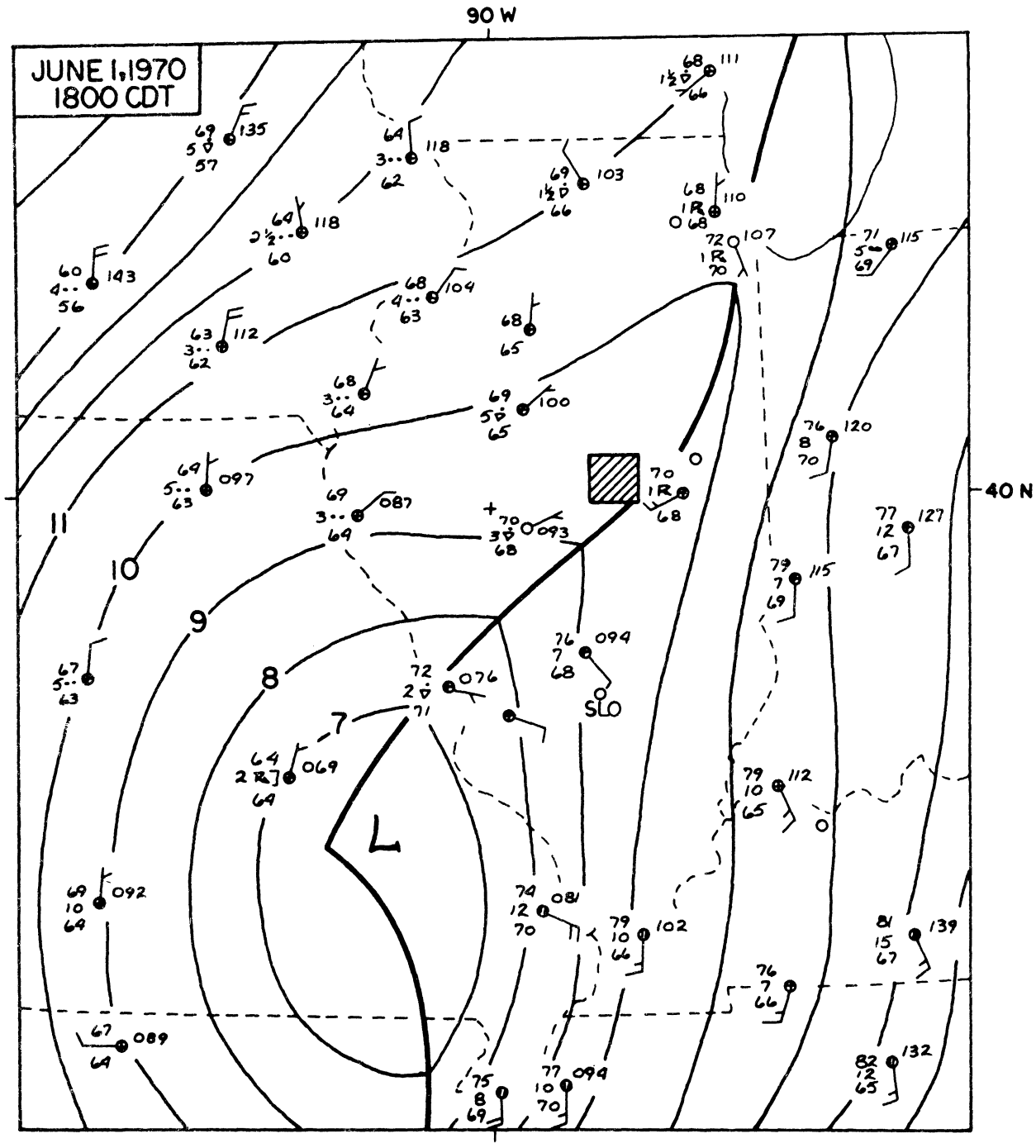

Fig. 5. Sea level sectional weather map, 1800 CDT, 1 June 1970

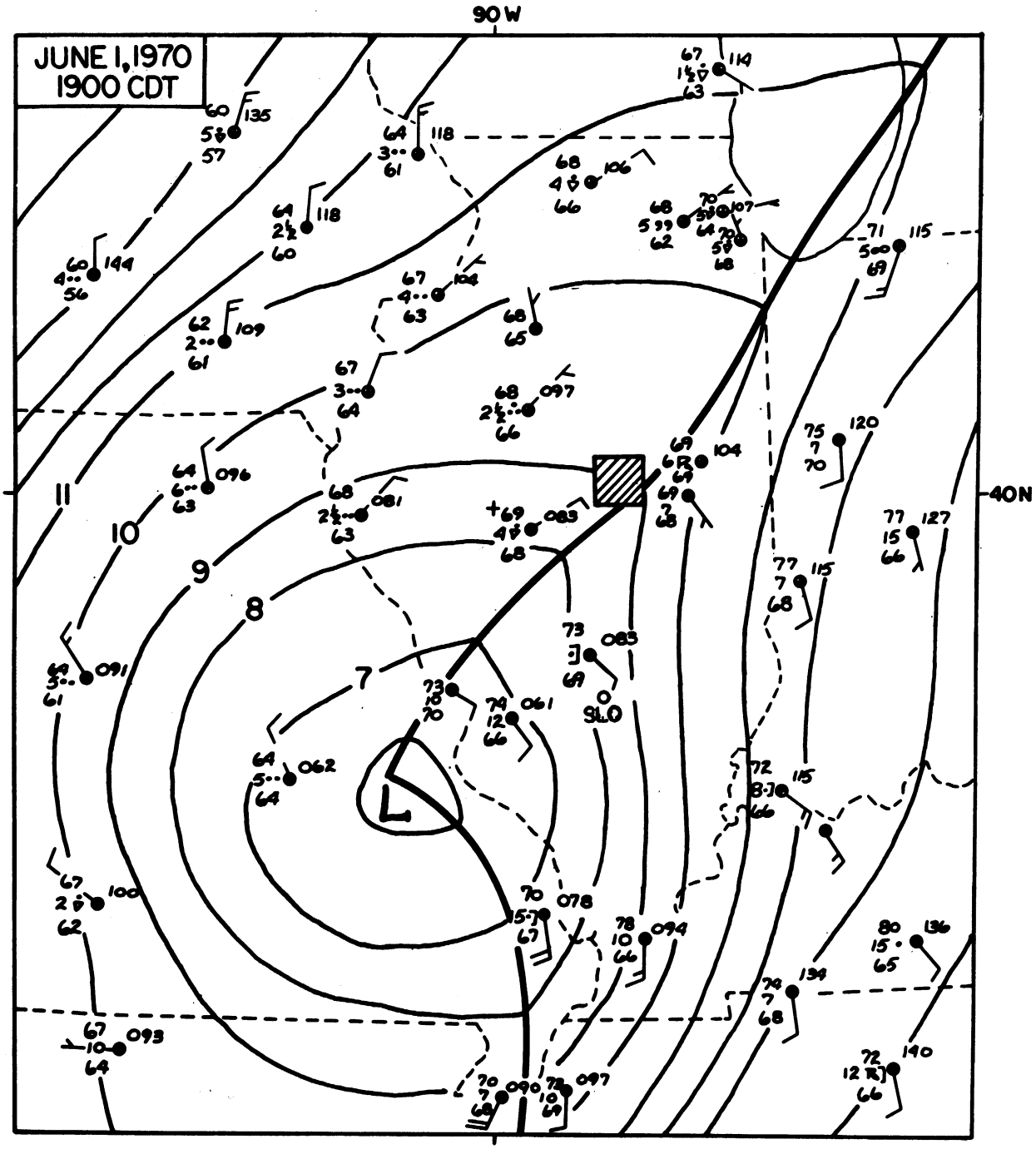

Fig. 6. Sea level sectional weather map, 1900 CDT, 1 June 1970

Salem (Fig. 7) is reasonably representative of the general air flow east of and above the frontal surface from 1639 to 1830. The Peoria sounding (Fig. 8) on the other hand, indicates the frontal surface near 650 mb (~3.5 to 4 km), but easterly to northeasterly flow only below about 900 mb (~1 km). This situation is quite similar to that reported by Fankhauser (1969).

The tracer was placed at 1900 ft MSL, or about 950 mb. Assuming an ordinary frictional (Ekmann) wind speed profile, we estimate the wind speed at this level to be ~1.1 km min^{-1}, and the wind direction to be about 5° E of S.

If we apply this translational velocity to the tracer cloud initially formed along the burn track (Fig. 9), the initial point, i, and the final point, f, are carried past the respective sequential sampling stations at the times indicated in Table 1.

Table 1. Wind Field Advection

Station	Tracer Cloud	
	i = initial point (see Fig. 9)	f = final point
G•2	1655	1706
G•1	1655	1707
M	1657	1709
G•3	1658	1710
M1	1708	1718
M2	1717	1728

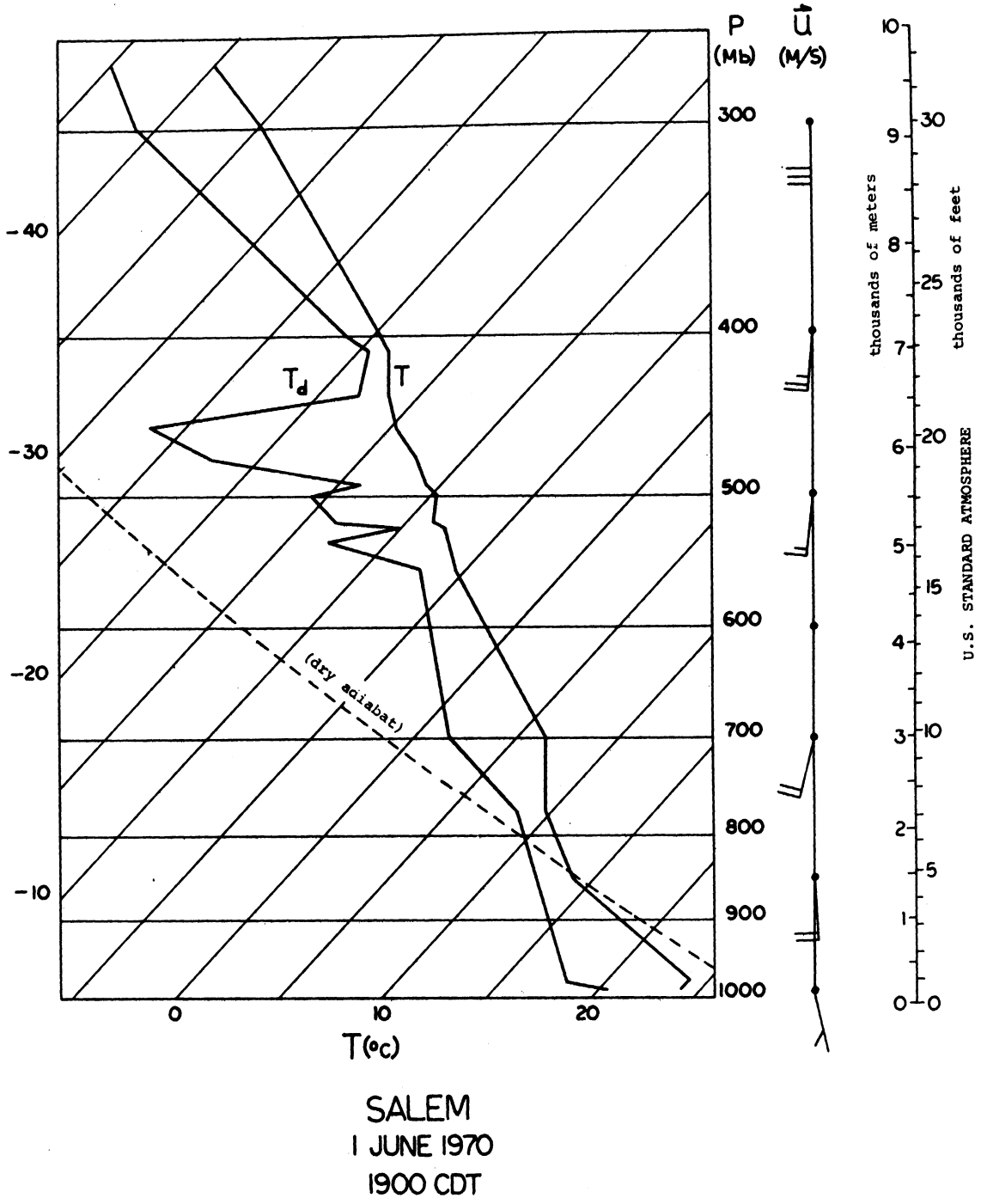

Fig. 7. Rawin sounding for Salem, Illinois, (SLO) 1900 CDT, 1 June 1970

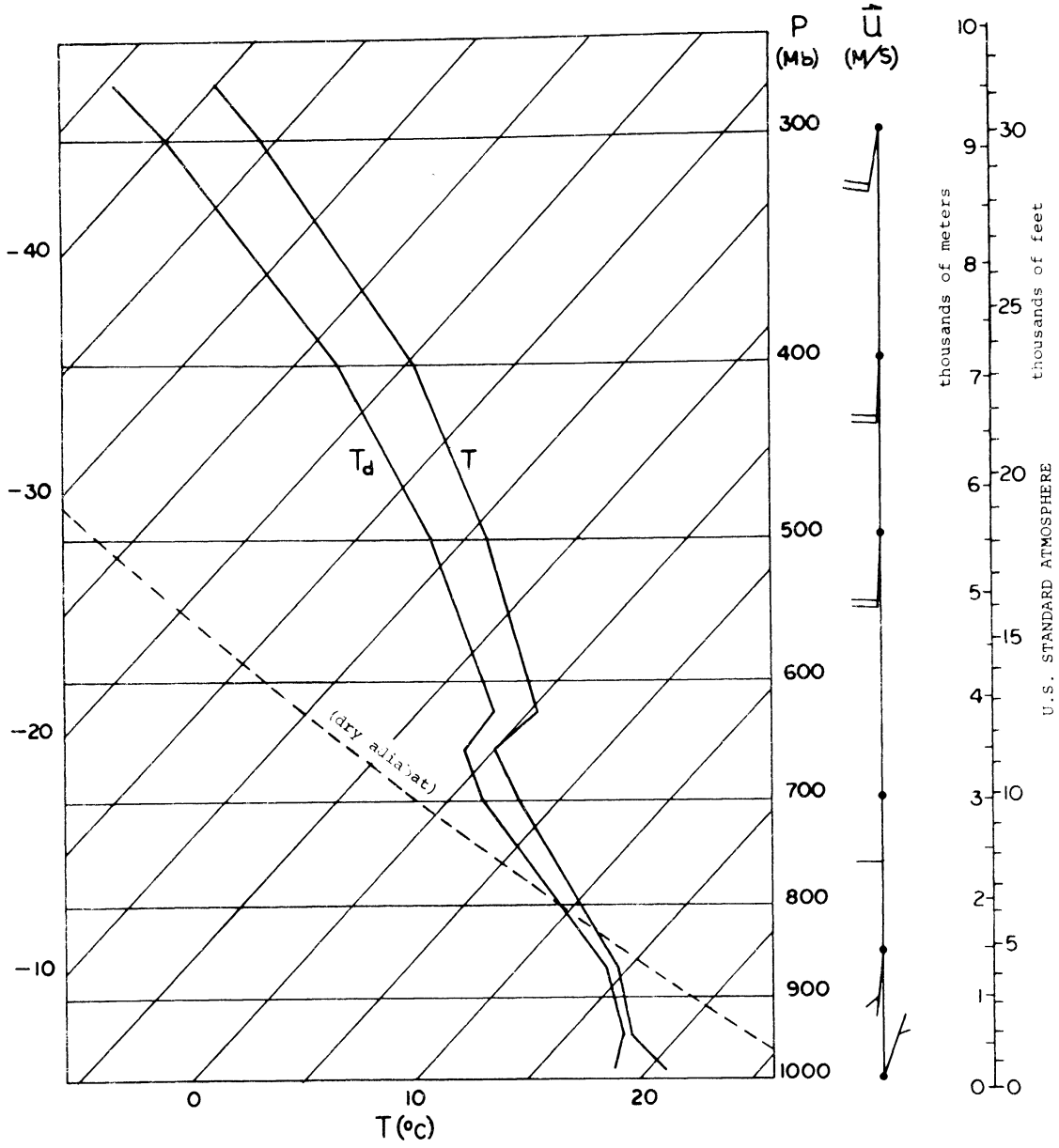

Fig. 8. Rawin sounding for Peoria, Illinois, (PIA)1900 CDT, 1 June 1970

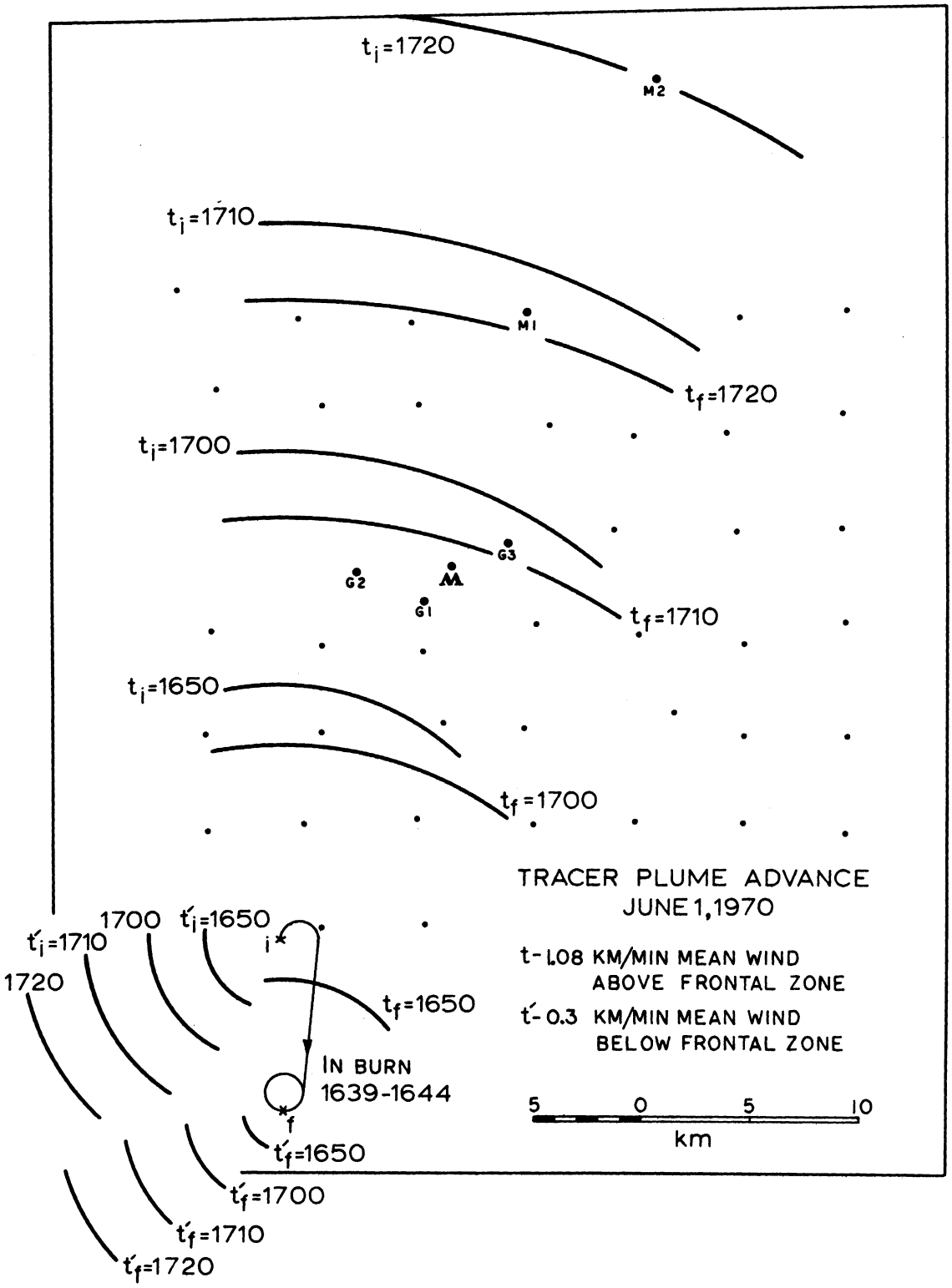

Fig. 9. Hypothetical isochrones of tracer cloud motion, 1 June 1970

Similarly, the mean wind velocity below the frontal surface is estimated to be ~0.3 km min^{-1} from northeast, and the isochrones in the lower left portion of Figure 9 indicate the times of arrival of tracer from points i and f of the burn track, respectively.

3. RADAR ECHO PROPAGATION

Referring to the radar echo centroid positions as shown in Fig. 10 and 11, mean velocities of propagation are given in Table 2.

Table 2. Radar Echo Propagation (see Fig. 10 and 11)

Track	Time Period	Mean Velocity Vector	
		Direction	Speed, Km min^{-1}
A	1639 - 1705	N 11° E	0.75
B	1639 - 1705	N 3° E	0.81
D_1	1655 - 1715	N 4.5° E	0.94
D	1715 - 1725	N 9.5° E	0.96
D_1	1710 - 1735	N 11.5° E	0.96
D_2	1730 - 1745	N 21° E	0.61

As noted previously (D) these echoes represent rain fields at 300 to 500 m altitude, i.e., very near the level of placement of the tracer (1900 ft MSL less 700 ft MSL altitude of CMI airport at which ISWS radar is located). Their motion represents the propagation of the estimated centroid of the most intense rain field at that level. Although the data are at best approximate, it appears that tracks A, B and D_2 indicate a tendency for the rainfield to propagate upwind somewhat, giving an effective motion slower than the mean wind

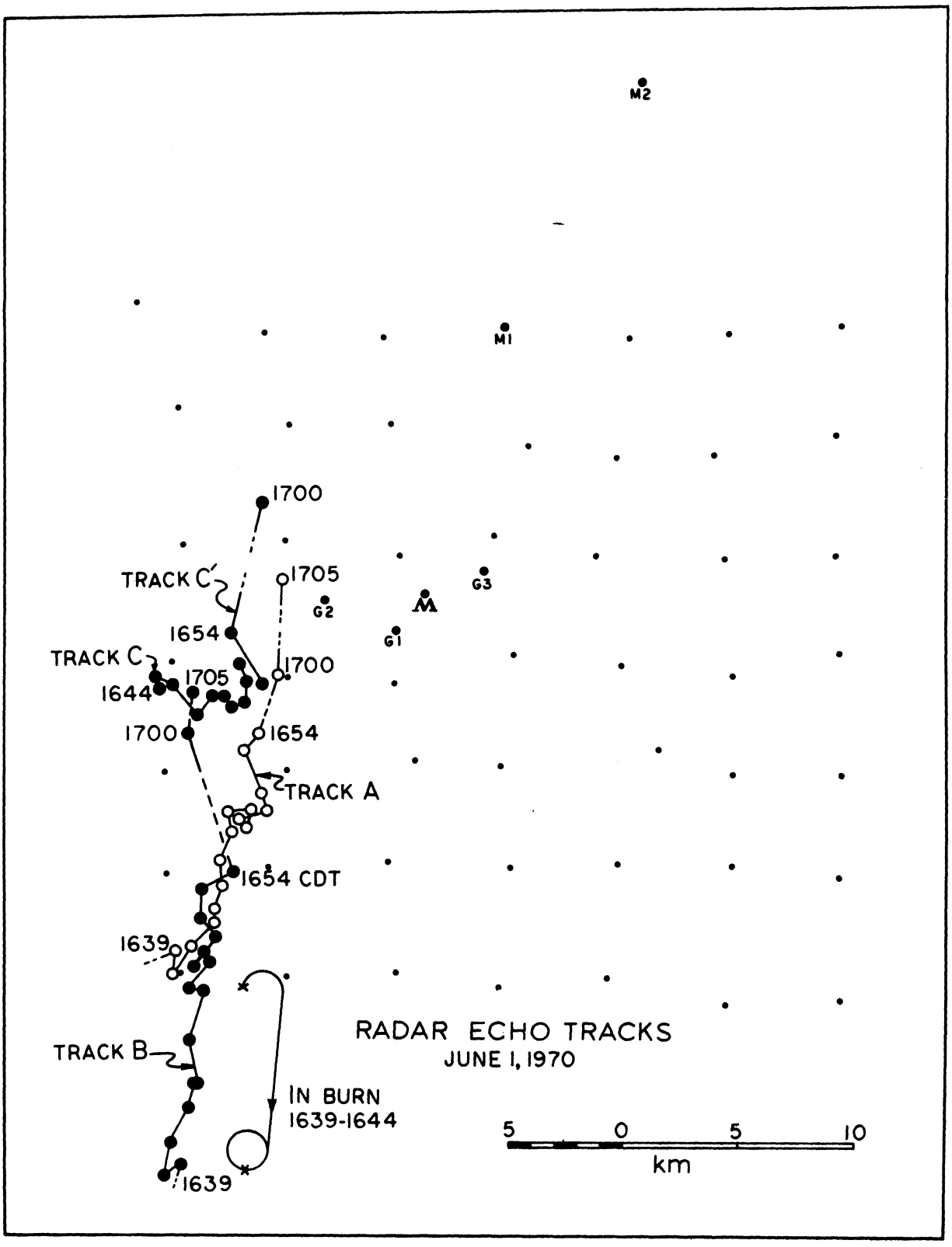

Fig.10. Radar echo tracks based upon estimated echo centroid positions, 1639 - 1705 CDT

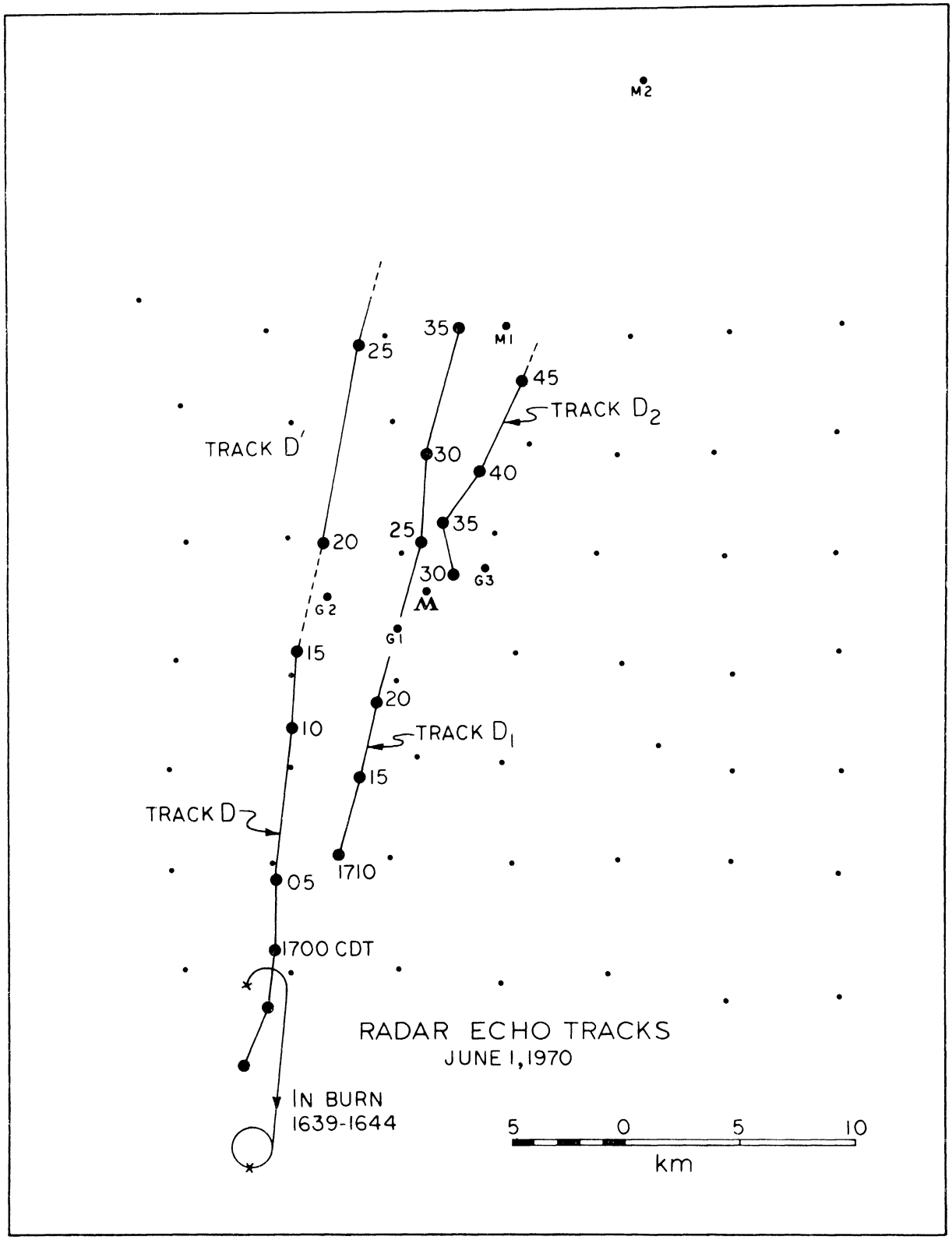

Fig.11. Radar echo tracks based upon estimated echo centroid positions, 1655-1745 CDT

field, and tracks D and D_1 indicate motion approximately at the speed of the mean wind. The echo propagation is, however, to the right of the mean wind vector in each case, ranging from 8° (track B) to 26° (track D_2). The short tracking period of only 15 min for the latter undoubtedly contributes to error of determination, so this value is considered somewhat tenuous.

4. RAIN FIELD PROPAGATION

The reduction of the ISWS raingauge data to simple total precipitation amounts leads to the rainfall distribution shown in Figure 12. The relation of these amounts to the tracer deposition is extremely tenuous if detectible at all. It is therefore clear that a more adequate treatment of the rainfall, relating it to the presence or absence of tracer at the time of the rainfall, etc., must be done if understanding is to be developed. The procedures described below were therefore devised.

After the indicated adjustment of all ISWS raingauge data to the same time base (CDT) as that used for the sequential rain samples, two series of charts were prepared to show the 10 min rainfall accumulations during the periods 1620 - 1840 and 1625 - 1845, respectively. Isopleths of rainfall amount in units of 10^{-2} in. were drawn at intervals in the geometric series represented by the powers of 2, i.e., at 1, 2, 4, 8, . . . hundredths of an inch, respectively. (Note that 0.8 in. per 10

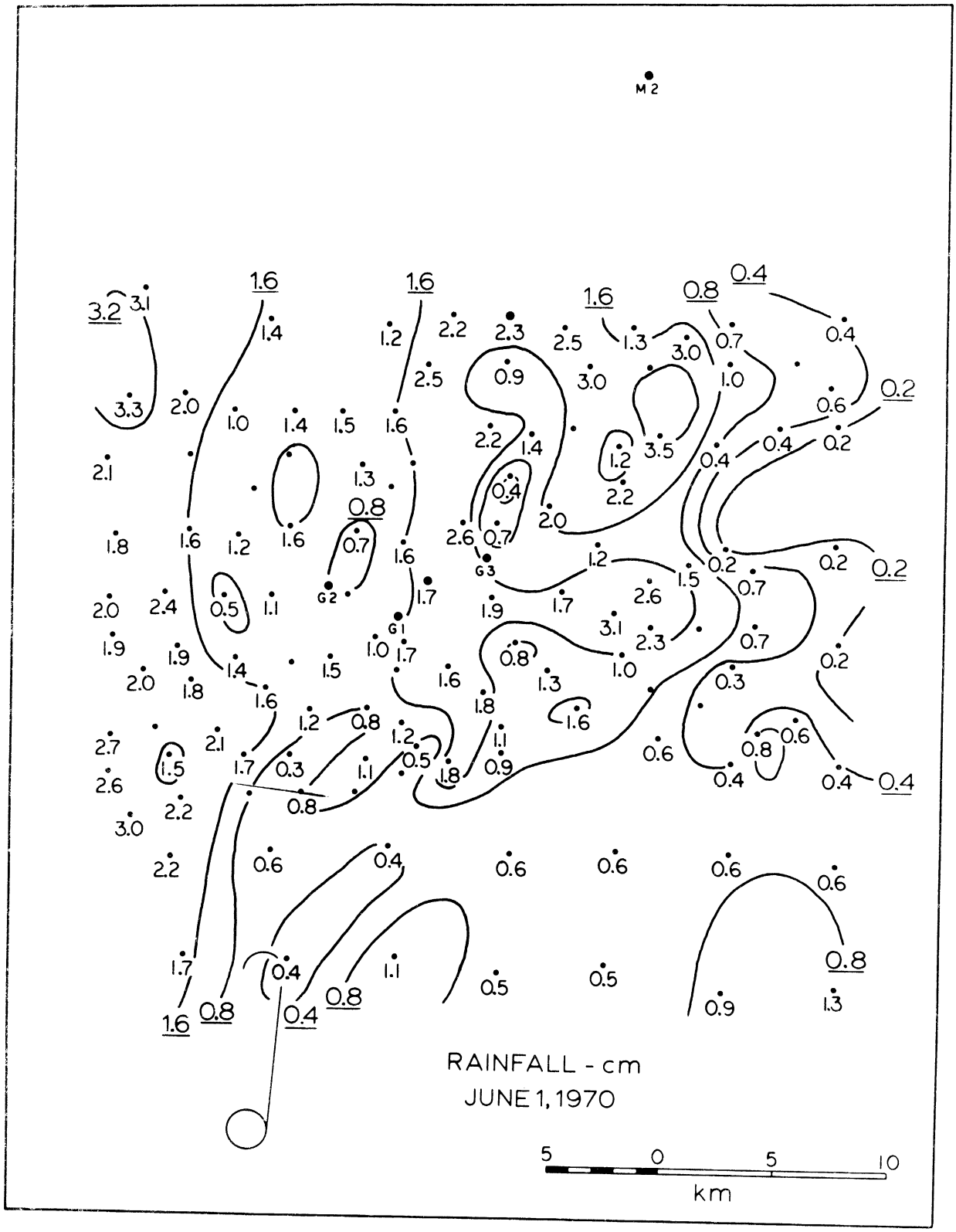

Fig.12. Total precipitation, 1 June 1970, from ISWS rain-gauge network

min = 12.2 mm hr^{-1}.) The average location and intensity of showers in the specified 10-min periods is thus resolved, and the intermediate (5-min displaced) analyses give a means of assessing the continuity of movement, development and dissipation of the individual showers. Representative charts from these two series are shown in Figures 13 and 14.

The propagation of the rain field was then depicted on graphic overlays by tracing off the estimated shower centroid (approximate center of most intense 10-min rainfall) and the isopleths of 12.2, 24.4, and 48.8 mm hr^{-1} mean rainfall rate from each of the 10-min-period charts (Figures 15 and 16). These rain field propagation charts show clearly the locus of all rainfall in excess of 12.2 mm hr^{-1}, and the progress of the isopleths and shower centers in time.

Starting at the southwest corner of the station network, rain of 12.2 but less than 24.4 mm hr^{-1} began between 1620 and 1625 CDT (Fig. 15). The propagation of this rain appears to have taken place at an uneven pace northward until 1645 (representing the period 1640-1650) when it turned toward northeast. The initial shower system (labeled I) appears to have maintained a fairly constant intensity, as indicated by the area enclosed by the 12.2 mm hr^{-1} isopleth and the absence of intensities as high as 24.4 mm hr^{-1}, for almost one hour (1620-1710). In the 1710-1720 period (plotted as 1715), the 24.4 mm hr^{-1} isopleth made its first appearance in an evidently new shower system that is designated II. This system then intensified in the next two 10-min intervals to give a 48.8

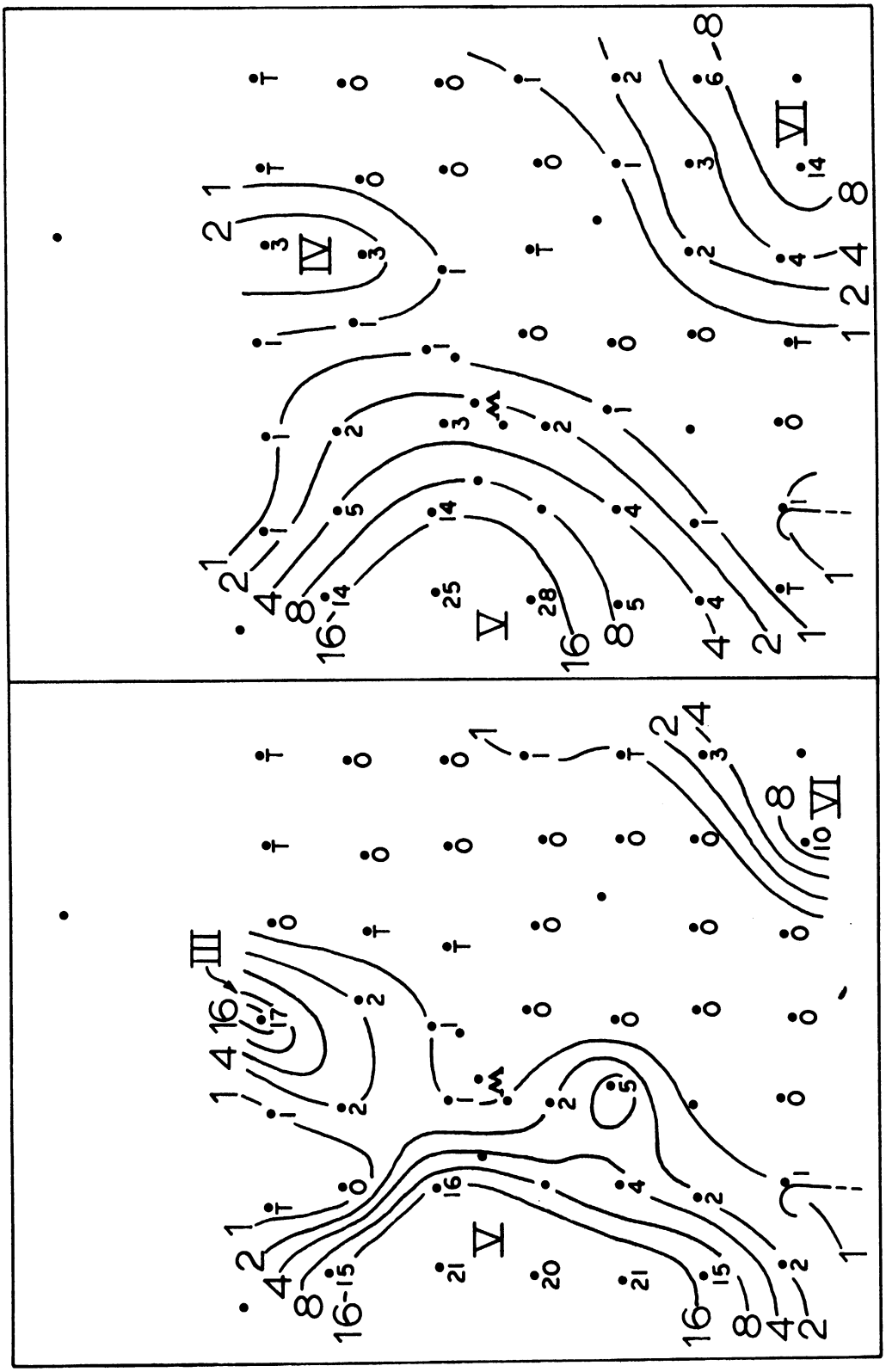

Fig.13. Sample 10-min rainfall distributions derived from ISWS raingauge data

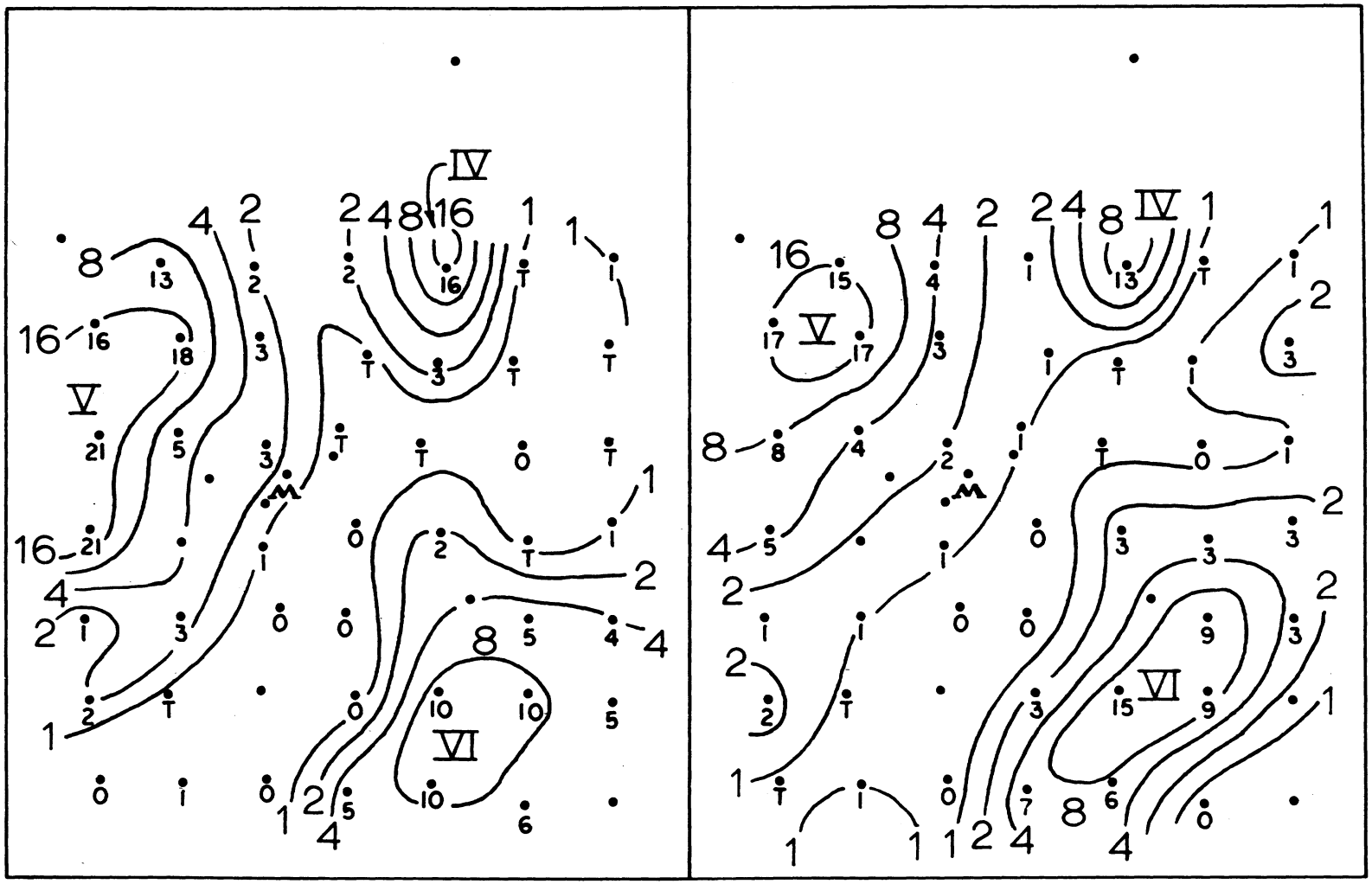

Fig.14. Sample 10-min rainfall distributions derived from ISWS raingauge data

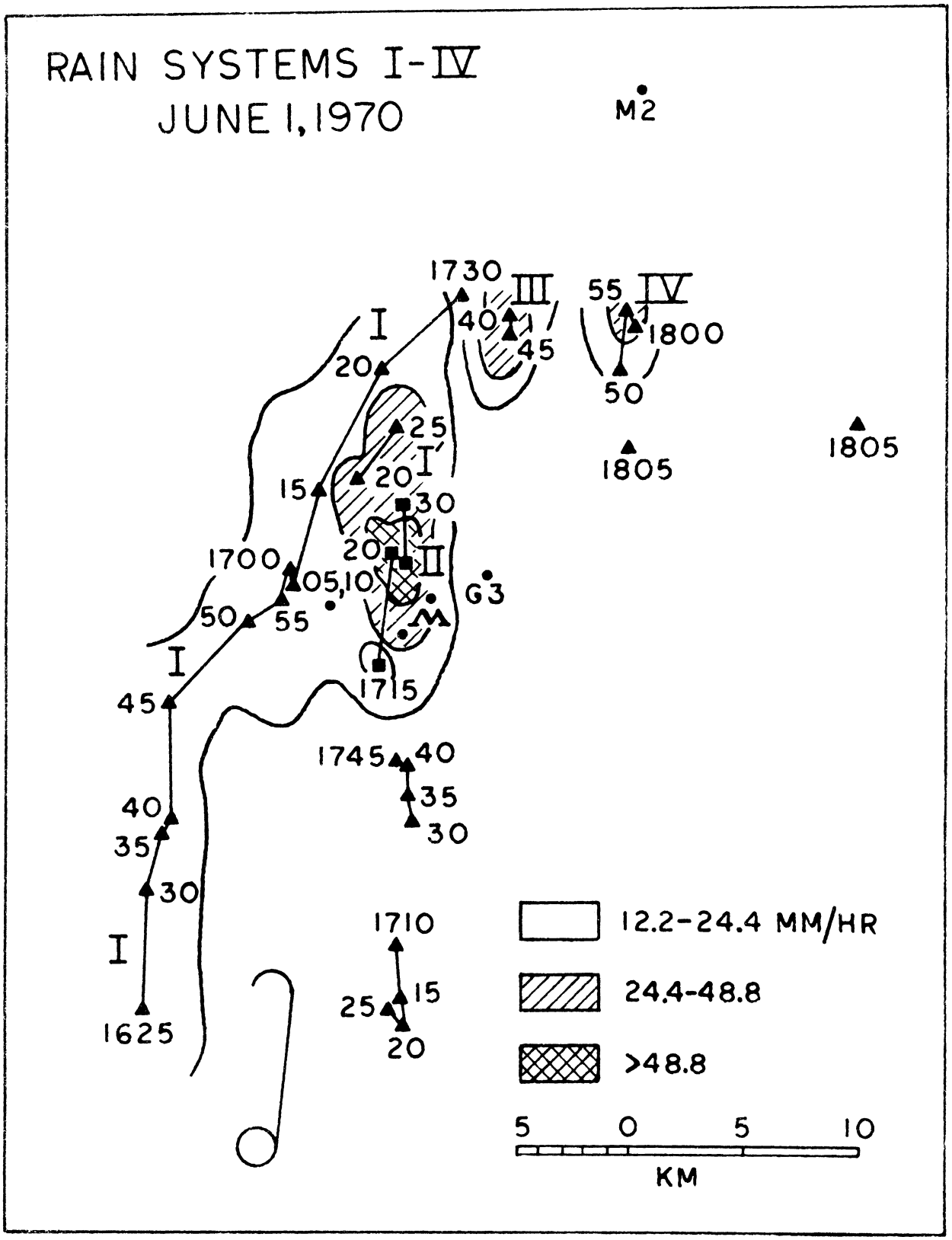

Fig.15. 10-min rainfall isopleth envelopes for systems I thru IV for the period 1620 to 1810 CDT, 1 June 1970

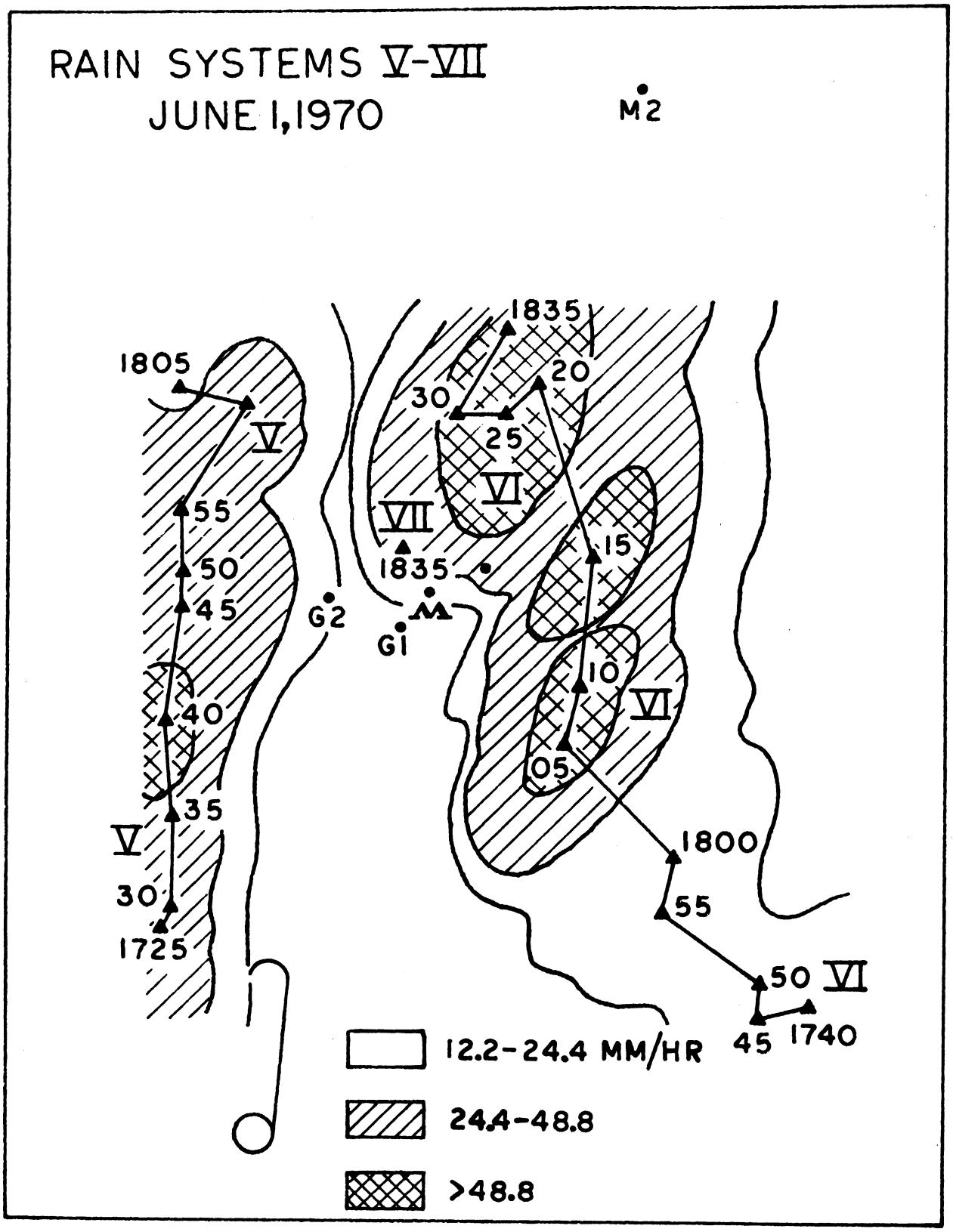

Fig.16. 10-min rainfall isopleth envelopes for systems V thru VII for the period 1720 to 1840 CDT, 1 June 1970

mm hr^{-1} isopleth, and vanished after about 1730. Two additional shower developments, III and IV, displaced successively eastward along the northern edge of the network, achieved ten-minute average intensities of 24.4 mm hr^{-1} at 1740-1745 and 1755, respectively, before dissipating or migrating off the network.

Meanwhile (Fig. 16), a new shower system, V, entered the network at the southwest corner at 1725, developed to 24,4 mm hr^{-1} intensity by 1730 and propagated nearly straight northward leaving the northeast corner of the network after about 1805. Again in this case, the intensity of the rainfall as represented by the 10-min averages appears to be remarkably constant from 1730 to 1800 except only for a brief surge to 48.8 mm hr^{-1} at 1740.

Finally (Fig. 16) the last shower system, VI, to affect the network on this date is first seen as a light shower (less than 12.2 mm hr^{-1}) at 1740 near the southeast corner of the network. It intensified to produce a 12.2 mm hr^{-1} isopleth by 1745, and then abruptly achieved 48.8 mm hr^{-1} at 1805 and persisted at this intensity until 1825, subsiding rapidly to 12.2 mm hr^{-1} by 1835 when a new development, VII, was observed some 7 km SSW of the apparent center of the old shower system. This system also is characterized by a propagation toward NNW, at considerable variance from the other systems, and from the radar echo propagation paths (Fig. 10,11).

This system was not recorded by the radar which was shut down at about 1745.

The deposition of indium tracer in the rain obviously depends upon the coincidence of the limited tracer cloud with the respective showers. We shall now turn to the estimation of the transport of the tracer cloud.

5. TRACER IN SEQUENTIAL SAMPLES

The sequential sampling stations provide an independent estimate of the rate of progress of the tracer cloud across the network. From reference D, (Figures 6-11 and Table 1), we have constructed Table 3.

Table 3. Timing of tracer-containing samples

Station	First tracer-containing rain sample	Last tracer-containing rain sample
G.1	~ 1712	~ 1745
G.2	~ 1712	~ 1830
G.3	~ 1725	~ 1733
M	~ 1715	~ 1730
M.1	~ 1725	~ 1750
M.2	~ 1750	~ 1814

This gives a leading edge transit time from G-1 to M2, a distance of 26 km, of about 38 min, and a resulting mean speed of 0.68 km min^{-1} for the leading edge of the tracer-bearing rain. The further computation of mean speeds from initial emission to the respective stations gives:

to G-1: 17 km, 33 min; .5.5 km min^{-1}
G-2: 17.5 km, 33 min; .53 km min^{-1}
G-3: 21 km, 51 min; .41 "
M : 19 km, 36 min; .528 "

M1: 31.3 km, 46 min; .68 km min^{-1}

M2: 43 km, 71 min; .61 "

Similarly derived figures for the trailing edge of the tracer-bearing rain are

from G-1 to M2:	26 km,	28 min;	.90 km min^{-1}
from endpoint to G-1:	25.3 km,	61 min;	.415 "
from endpoint to G-2:	25.8 km,	121 min;	.21 "
from endpoint to G-3:	29.3 km,	49 min;	.60 "
from endpoint to M:	27.3 km,	46 min;	.59 "
from endpoint to M1:	39.6 km,	66 min;	.60 "
from endpoint to M2:	51.3 km,	90 min;	.57 "

Summary:

(a) Tracer-tagged rain arrived at stations G·2 and G·1 at about the same time initially;

(b) tracer-tagged rain reached stations G·3 and M1 at about the same time although M1 is situated 11 km downstream (north) of G·3;

(c) tracer-tagged rain was received at station G·2 for some time after it had stopped appearing at the other stations;

(d) transit times for the beginning and end points of the tracer imply a mean speed in the range 0.52 to 0.68 km min^{-1}; the higher speed of 0.90 km min^{-1} for the advance of the trailing edge of the tracer from G·1 to M2 probably reflects a delay of rainfall at G·1; this implies an overall mean transit speed close to 0.60 km min^{-1};

(e) the direction of the mean transit inferred above is slightly east of northward, and appears to curve eastward at the greater

distances; this, together with the lithium (also sodium, magnesium and potassium) transport data (Semonin, 1970) further suggests that the transport of the tracer at the greater distances was strongly affected by winds characteristic of the 3 to 4 km levels. Recall that the lithium was emitted over a descending burn path, but mainly near 14,000 ft MSL (~4 km), and that it was deposited northeastward from the ignition point;

(f) the eastward advance of tracer south of station M was sharply limited, whereas large amounts of tracer material were deposited westward of the burn track beyond the limit of the sampling network;

(g) the appearance of tracer as late as 1830 at station G·2 is indicated in (D, Fig. 8). This is a dilute sample, but was preceded by more than 90 min of continuous rain. It is well above the trace concentrations found in all other samples at this late hour. The rain field analysis gives the first indication as to how the tracer could have been brought down this late: we infer that it came to the area in system V (Fig. 16) rainfall, and that the principal part of the tracer deposition along the western edge of the network was also carried by this system. This requires the further inference that a substantial quantity of indium was carried downward and westward with the low level currents predominating below the frontal surface. This material was then drawn into system

V convective cells as they entered the area. It appears that systems VI and VII must have been unmarked by the indium release;

(h) tracer observed at station M•2 as late as 1814 appears to have been associated with systems III and/or IV, and transferred more or less directly with the flow field above the frontal surface. The average transport velocity of about 0.6 km min^{-1} contrasts with the general wind speed of about 1.1 km min^{-1}, and suggests that the horizontal projection of the tracer trajectory was considerably longer than the straight line distance.

B. An Interim Report on
Polynomial Fit of Mason's Table of
Collision Efficiencies

Abstract

For numerical simulation of rain generation and contaminant removal processes, it is necessary to have values of the collision efficiencies for raindrops on smaller droplets and particles in free fall. The table compiled by Mason (1971) is relatively authoritative, but even so, because of both editorial oversights and theoretical disunities, the values it contains tend to be somewhat oscillatory and in certain areas, at odds with one another. Thus this table as it stands is not satisfactory for numerical simulation work: it requires smoothing so that valid interpolation can be made.

Storebø and Dingle (1973) smoothed part of this table of values graphically to meet immediate requirements, but caution that theirs is only an interim answer to the problem. In the present paper we describe efforts that we have undertaken to devise a more satisfactory solution. To date these efforts are entirely empirical, and the results fall short of the standards we should like to attain in terms of accuracy and of simplicity of expression.

Polynomial Fit of Mason's Table of Collision Efficiencies

An Interim Report, May 1973

I. INTRODUCTION

A fundamental process in the growth of raindrops and the removal of atmospheric particles is that of collision-coalescence. A falling drop will collide with and collect droplets and particles in its path; because of the aerodynamic flow around the drop and surface film effects, not all collisions will result in collections. The fraction of particles in the path of the drop which collide with the drop is the collision efficiency. The fraction of those particles which then merge with the drop is the coalescence efficiency. The product of the two is known as the collection efficiency.

In the laboratory, the collection efficiency has been studied by means of photography, by weighing drops after falling through an environment of droplets, and by other techniques. Theoretical calculations have been made to obtain estimates of the collision efficiency; coalescence efficiencies are not well known and are most frequently assumed to be unity.

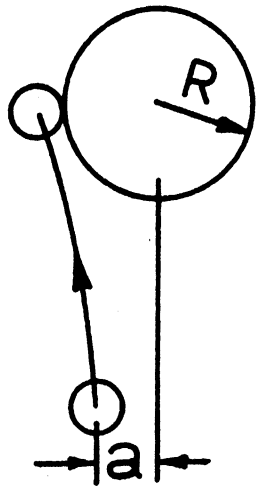

Figure 17

Figure 17 shows the path of a droplet relative to a large drop in free gravitational fall. Langmuir and Blodgett (1946) calculated the grazing trajectories of various drop-droplet pairs, thus determining the value of a, by means of an interpolation formula to span the interval between the potential flow and the viscous flow theoretical ideals.

For a collector drop of radius R and a collected droplet of radius r, the collision efficiency E' was originally defined (Langmuir, 1948) as the ratio of the collision cross section to the geometric cross section of the collector drop essentially neglecting r in comparison with R. Hence

$$E' = \frac{\pi a^2}{\pi R^2} = \frac{a^2}{R^2}$$

It is apparent from Figure 17 that E' can be as large as 4.0 when $r \to R$. More recently (Das, 1950; Ludlam, 1951) the collision efficiency has been redefined to account for the size

of the collected droplet:

$$E = \frac{a^2}{(R + r)^2}$$

In this case, $E \leq 1.0$.

Still later, Shafrir and Neiburger (1963, 1964) introduced the term linear collision efficiency, $y_c = a/R$; $(y_c \leq 2.0)$.

Because of the variations in the representation of the collision efficiency, it is important to understand which expression an individual author is using. The calculation of the collection kernel, K (Berry, 1967), which is related to the growth of the collector drop, depends on the definition of the collision efficiency used. Thus, (if the coalescence efficiency is equal to unity),

$$K = \pi(R + r)^2 E \Delta v = \pi R^2 E' \Delta v = \pi R^2 y_c^2 \Delta v = \pi a^2 \Delta v$$

where Δv is the fall speed of the collector drop relative to the collected droplet. Throughout the present study the term "collision efficiency" is used for $E = a^2/(R + r)^2$.

To date, the best and most comprehensive table of collision efficiencies is that compiled by Mason (1971). This tabulation (Table 4) is derived from the following: Hocking and Jonas (1970) for $R \leq 30\mu$; Shafrir and Neiburger (1964) for $30\mu \leq R \leq 100\mu$; and Fonda and Herne (1957) for $R > 100\mu$.

Table 4. Collision efficiencies for drops of radius R colliding with droplets of radius r at 0°C and 900 mb. (After Mason, 1971)

	r(μm)							
R(μm)	2	3	4	6	8	10	15	20
15		0.003	0.004	0.006	0.010	0.012	0.007	-----
20	0.002	0.002	0.004	0.007	0.015	0.023	0.026	-----
25	-----	-----	-----	0.010	0.026	0.054	0.130	0.06
30	-----	-----	-----	0.016	0.058	0.17	0.485	0.54
40	-----	-----	-----	0.19	0.35	0.45	0.60	0.65
60	-----	-----	0.05	0.22	0.42	0.56	0.73	0.80
80	-----	-----	0.18	0.35	0.50	0.62	0.78	0.85
100	0.03	0.07	0.17	0.41	0.58	0.69	0.82	0.88
150	0.07	0.13	0.27	0.48	0.65	0.73	0.84	0.91
200	0.10	0.20	0.34	0.58	0.70	0.78	0.88	0.92
300	0.15	0.31	0.44	0.65	0.75	0.83	0.96	0.91
400	0.17	0.37	0.50	0.70	0.81	0.87	0.93	0.96
600	0.17	0.40	0.54	0.72	0.83	0.88	0.94	0.98
1000	0.15	0.37	0.52	0.74	0.82	0.88	0.94	0.98
1400	0.11	0.34	0.49	0.71	0.83	0.88	0.94	0.95
1800	0.08	0.29	0.45	0.68	0.80	0.86	0.96	0.94
2400	0.04	0.22	0.39	0.62	0.75	0.83	0.92	0.96
3000	0.02	0.16	0.33	0.55	0.71	0.81	0.90	0.94

2. PROCEDURE AND RESULTS

When one examines this table by plotting the values and striking isopleths through the graphic field (Figure 18), a number of irregularities come to light: (a)some values appear to be editorially in error, e.g., values for (R,r) = (300,15) and (300,20) and for (1800,15) and (1800,20); (b)some series of values appear to oscillate as if a computational rather than a physical source were involved. Such an oscillation is observed in the original results of Shafrir and Neiburger, but it is not explained by them. In summary, so that suitable interpolation values can be obtained for numerical simulation of drop growth and particle attachment processes, it is necessary to smooth the values of Table 4. Storebø and Dingle (1973) performed a direct graphic smoothing and note that theirs is intended only as an immediate interim solution.

It is the objective of the present effort to achieve a more satisfactory resolution of this problem. The solution required is a well-fitted collision efficiency surface expressed in terms of r and R.

The collision efficiency surface has a complicated shape which is not readily expressed in terms of easily recognized functions. Berry (1967) proposed the following form for the linear collision efficiency, y_c, defined and computed by Shafrir and Neiburger (1964):

$$y_c = A + Bp + \frac{D}{p^F} + \frac{E}{(1 - p)^G}$$

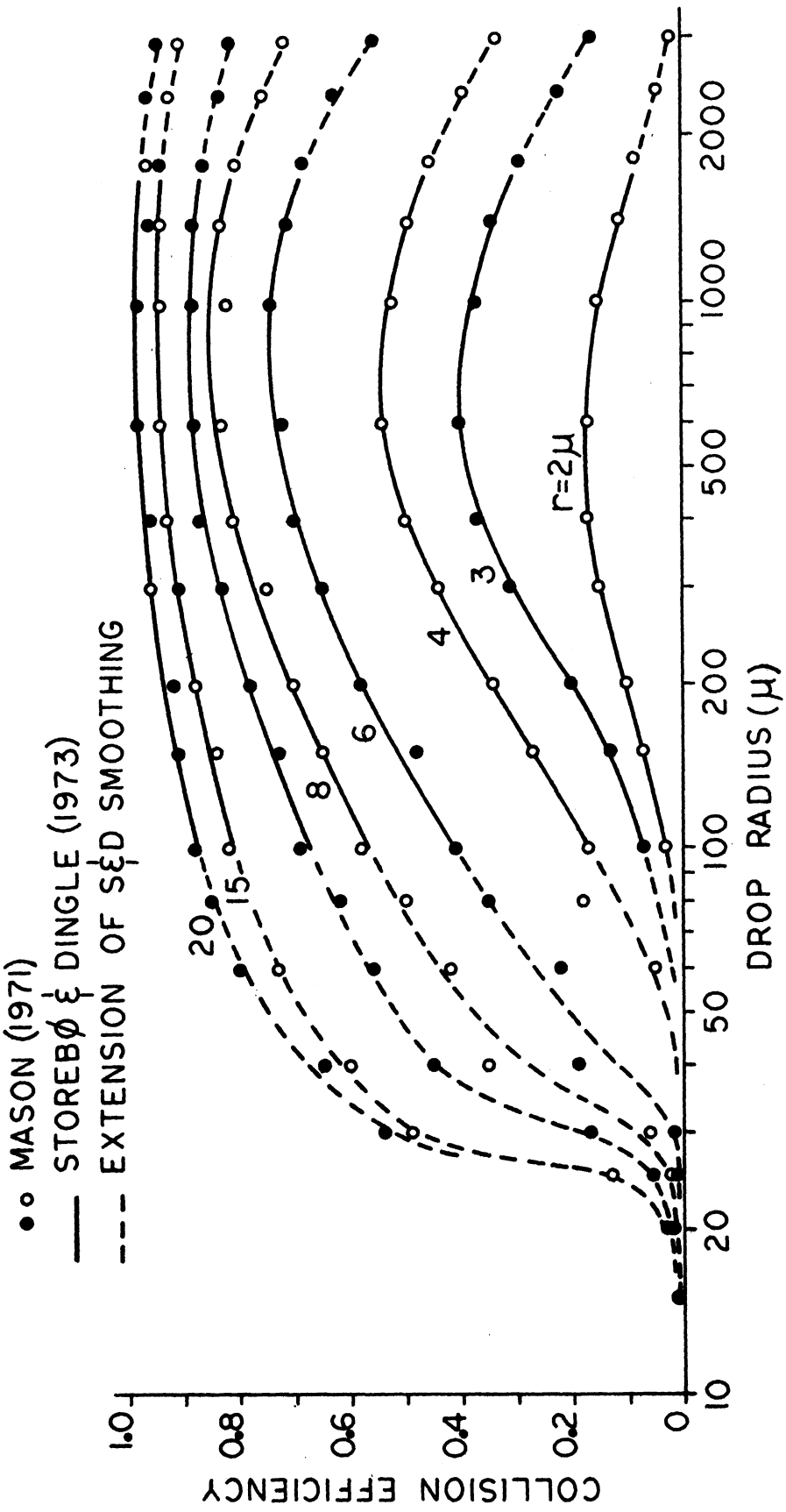

Fig.18. Collision efficiencies according to Mason (1971)
Freehand smoothing by Storebø & Dingle (1973) for
$100\mu \leq R \leq 1700\mu$

where p = r/R and D, E, F, G are functions of R. The limitation to Reynolds numbers of 19.2 and less restricts Shafrir and Neiburger's results to a maximum collector drop of 136μ radius, and Mason has selected their values to represent the range $30\mu \leq R \leq 100\mu$. A comparison of Mason's tabular values against curves computed by Berry's formula is shown in Figure 19. The uneven variation of the Mason values is evident. The limited range of application of these data restricts them mainly to cloud droplet coalescence processes; our interest is directed more toward the raindrop size domain ($100\mu \leq R \leq 3000\mu$).

By means of a statistical routine, the best fit polynomials in r and R were computed to predict E as represented in Table 1. Values of E and of the mean square deviation from the tabulated values were obtained as output. The initial effort was directed to generating a surface to represent the entire data field, but this did not prove feasible. Later attempts were restricted to the range $R \geq 100\mu$. This part of the table is entirely drawn from the work of Fonda and Herne (1957), hence the problems of transition between sources was obviated. Further, this is the range of greatest interest for the rainfall impact-collection process.

The best result of these efforts is a third degree polynomial in r and ℓn R which yields the predictions shown in Figure 20. The inflections in the curves for $r = 2\mu$ and 3μ are not reproduced, and some negative values are found for $r = 2\mu$.

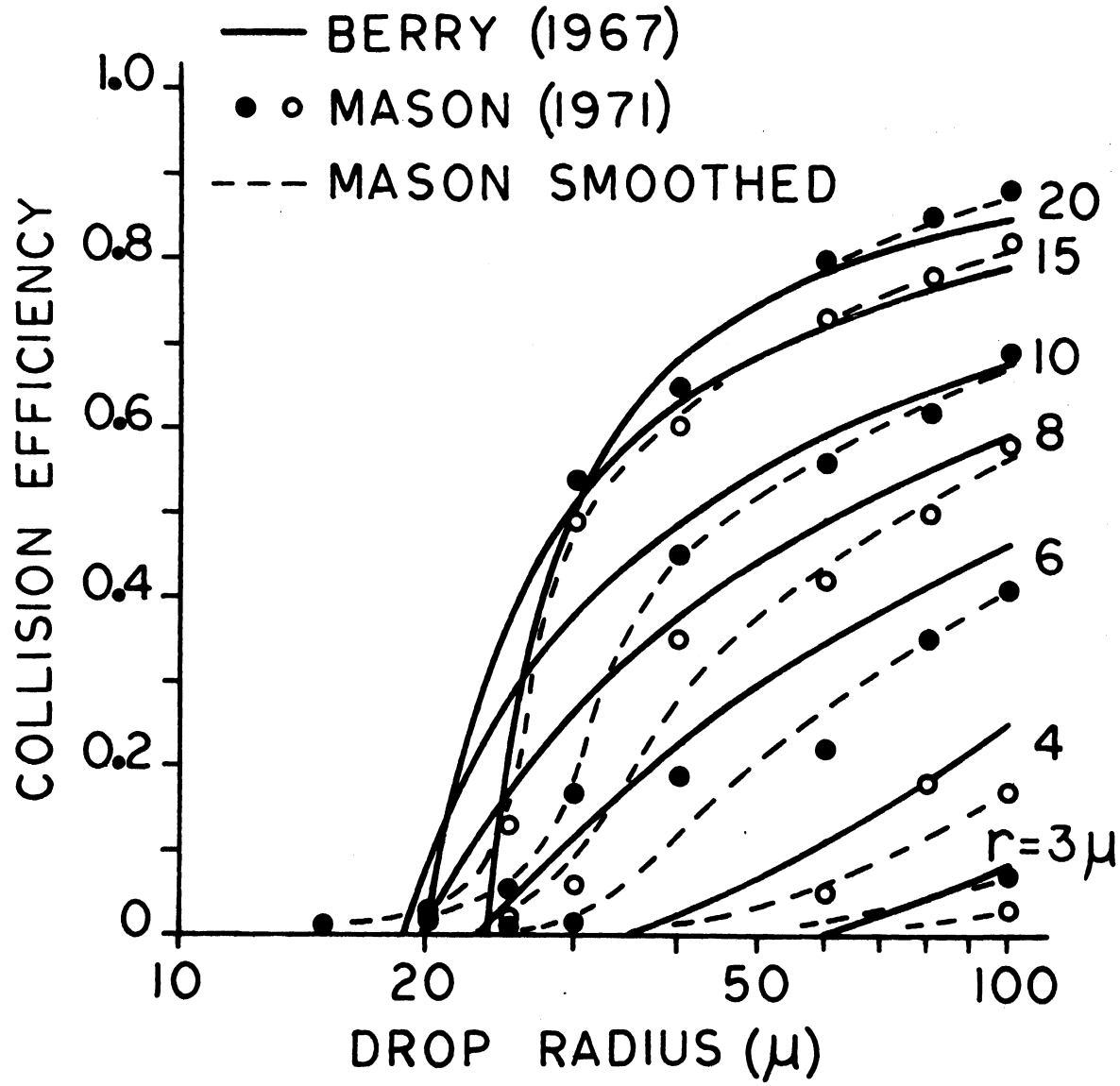

Fig.19. Berry's (1967) analytical representation of the collision efficiencies of Shafrir & Neiburger (1964). Mason's (1971) tabulated values are shown for comparison.

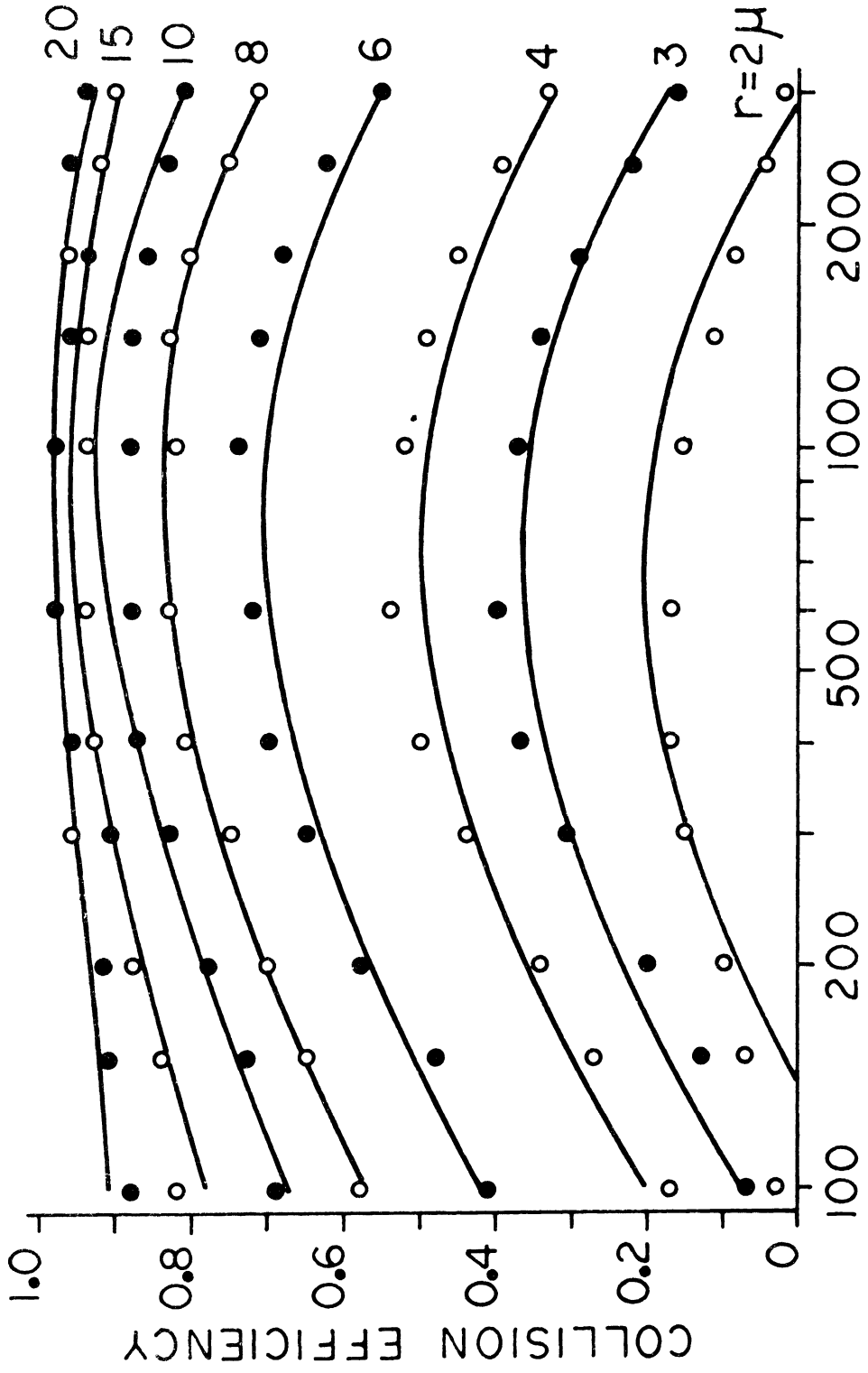

Fig.20. Representation of Mason's (1971) table of collision efficiencies by the polynomial Efficiency = $a + br + c\ell nR + dr\ell nR + e\ell n^2R + fr^2 + gr^3 + hr\ell n^2R + jr^2\ell nR + k\ell n^3R$

It was found that the residuals can be reduced somewhat by arbitrarily adding some periodic functions, but the physical validity of this measure is questionable.

A fourth degree polynomial in ln r and ln R (Figure 21) gives the best fit for small values of r, but predicts a crossing of the curves for r = 15μ and 20μ. This result is not acceptable without further analysis. Similar efforts in the domain $R \leq 100$ also yielded unsatisfactorily large mean square residuals.

An alternative approach to the problem is to smooth over the range of one independent variable at a time. This was done by fitting a polynomial to each of the r-isopleths in the R vs E plane and then fitting another set of polynomials to the coefficients of the first set. This yielded no improvement.

Currently a third approach is under study. This is Prony's method (Lanczos, 1956; Whittaker and Robinson, 1924) which fits data to a series of exponentials. Obvious difficulties arise in (a) a need for initial accuracy of the data and (b) the appearance of complex expressions in the solution.

3. CONCLUSION

Because of the requirement to use collision efficiency values in rain field calculations, a rational smoothing technique for the tabulated collision efficiency data is required. Direct empirical fitting of Mason's (1971) table fails so far

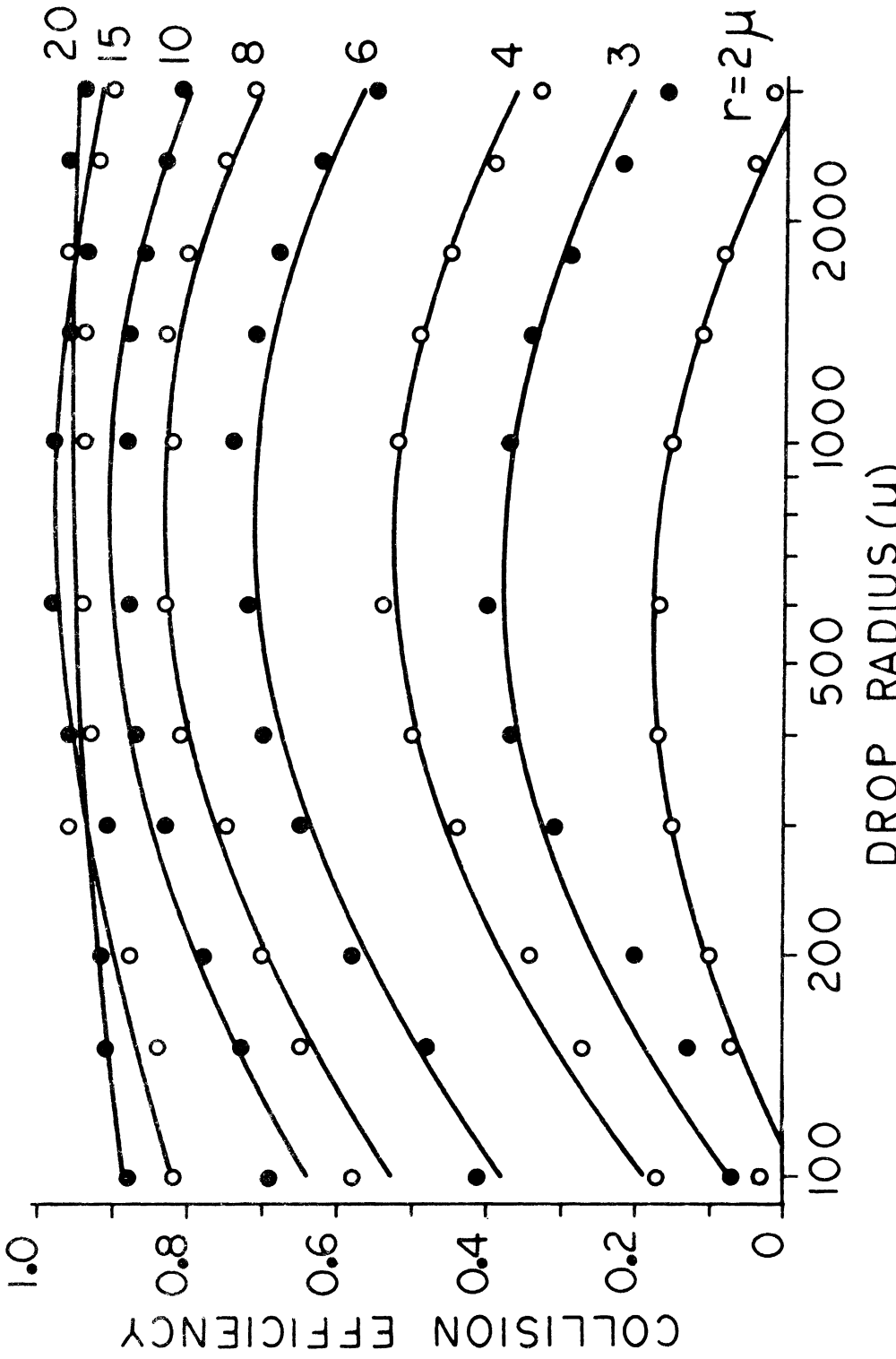

Fig.21. Representation of Mason's (1971) table of collision efficiencies by the polynomial Efficiency = $a + b\ell nR + c\ell n^2R + d\ell nr + e\ell n^2r + fr\ell nR + g\ell nr\ell nR + h\ell nr\ell n^2R + jr\ell n^2R + k\ell n^2r\ell n^2R$

to yield an adequate solution. Part of the difficulty lies in the fact that the basic data are somewhat in doubt. Another part of the difficulty is in the proper selection of suitable terms for the fit equations. It therefore appears that a more complete physical analysis of collision must provide the basis from which to solve this problem. An interim answer lies in a simple interpolation procedure applied to a crudely smoothed table of collision efficiencies as is done, e.g., by Storebø and Dingle (1973)

C. Progress in Modeling of the Rain Scavenging Processes

Several different activities and approaches have been brought to bear upon our modeling effort. Among these are (1) an analytical approach being pursued as a doctoral problem by Mr. Y. Lee, (2) the numerical simulation of nucleation of cloud droplets upon mixed nuclei following a specified atmospheric path, (3) an effort to formulate drop-on-droplet or-particle collision efficiencies in a form suitable for numerical integration of washout, (4) an empirical formulation of terminal fall speeds of raindrops. Of these efforts, Mr. Lee's progress is reported below and in Section III, and (4) is reported among our published papers (Section IV), whereas (3) is reported above. Work on (2) has gone forward rapidly under a sabbatical project and subsequent classroom and research efforts, and is reported briefly here. A paper derived from this work has been submitted for publication and is included in Section III below.

It is clear that the scavenging function of precipitation is intimately related to the primary cloud- and rain-producing processes, and that a key process here is that of the nucleation of the vapor-liquid phase change. To this date, the nucleation of droplets upon airborne salt (NaCl) particles has been treated by several investigators: Howell (1949), Mordy (1959), Neiburger and Chien (1960). More recently the chemical formulation of the problem has been clarified and simplified for numerous

inorganic salts by Low (1960). The importance of ammonium sulfate as airborne nucleating material has been pointed out by numerous workers (e.g., Twomey, 1971; Mason, 1971; Scott and Hobbs, 1967; Fitzgerald, 1973), but relatively little work has been done on mixed nuclei containing only a fraction of hygroscopic mass. Junge and McLaren (1971) studied the relation of aerosol size spectra and composition to cloud nuclei spectra. They show that the size of the nucleus in each case is a much more important factor than the proportion of soluble salt in the nucleus, down to 10^{-3} by volume. Fitzgerald (1973) essentially confirms that conclusion and gives an estimate of the fraction of soluble material in natural aerosol samples between 15 and 35%.

Another limitation of much of the cloud droplet growth modeling cited above is the consistent assumption that the growth equation at equilibrium, essentially as derived from Mason (1957) adequately expresses the process envisaged. Storebø and Dingle (1973) chose a somewhat distinct approach to the problem. They argue that despite the small relaxation times characteristic of cloud droplets, the process of condensation growth is not an equilibrium process, and for some situations, it may be important to allow the deviations from equilibrium to operate. To this end they devised a model of nucleation and droplet growth in which the vapor and heat transfer processes are controlled only by the appropriate diffusivities and time.

The results of these computations, made along an orographic trajectory, do not differ greatly from the results from equilibrium computations at comparable lift rates (up to 15 cm/sec). The extension to higher rates of ascent remains to be done.

One result,which may be especially significant for the non-equilibrium computations, is noted in connection with a brief descent which follows a more sustained ascent period. Here, after about 30 m of descent, the non-equilibrium computations show that the smaller droplets have evaporated restoring their nuclei to pre-nucleation sizes, whereas the larger droplets have lost their acquired water more slowly. If one now envisages a renewal of lifting, it appears that the cloud droplet size distribution will be broadened. This bears upon the important question of the evolution of broadened droplet size distributions in cumulus congestus and cumulo nimbus clouds (see, e.g., Weickmann and aufm Kampe, 1953; Warner, 1969a). Although the question of spectral broadening associated with the entrainment of environmental air has been studied by several investigators (Mason and Chien, 1962; Warner, 1969a), the effect of alternately rising and descending motions, as should be expected in the eddy circulation in cumuli, has been treated (Kornfeld, 1970) only in terms of the equilibrium growth equation. More recently Paluch (1973) has applied the equations used by Kornfeld (1970) and Warner (1969b) in

studies of wave clouds and finds that the alternate condensation-evaporation processing may lead to considerable spectral broadening which varies with the frequency and amplitude of the alternations. The non-equilibrium computations are expected to accentuate this effect.

In brief, therefore, despite a rather long history of computational modeling, it appears that the nucleation and growth of cloud droplets upon nuclei of mixed and various composition deserves still further work.

From the outset it has been clear that all of these processes in cumuli depend upon, and feed back effects upon, the circulations in the convective cells. The approach of the atmospheric dynamicists has always been that of modeling convection by means of the dynamical equations usually omitting condensation-evaporation, but at best parameterizing them. In our view, these efforts have yielded reasonable results for one- and two-dimensional models. However, the three-dimensional models required for an adequate treatment of convective circulations remain in a primitive state primarily because of their excessive requirements of computer capacity (Lilly, 1970; Steiner, 1972). In particular, it appears at present impractical to model turbulent convection in the motion scales required for an adequate treatment of the phase changes in cumuli.

Approaching the problem as a cloud physicist, however, it appears that an equally valid approach to the above might be to model the condensation-evaporation processes physically, treating the trajectories of the particles by means of appropriate parameters, and combining the products statistically in accord with sound descriptive knowledge of cumuli. The adaptation of the Storebø-Dingle model to this approach is quite direct. Characterizations of convective storms and clouds such as those provided by Fankhauser (1969, 1971) and Ackerman (1967), for example, afford the means of evaluating suitable trajectory parameters for cloud and rain-drops within the cloud. It is anticipated that relevant results may be obtained by this approach more promptly than by the aerodynamic one.

D. References for Section I

Ackerman, B., 1967. The nature of meteorological fluctuations in clouds. J. Applied Meteor., 6, 61-71.

Berry, E. X., 1967. Cloud droplet growth by collection. J. Atmos. Sci. 24, 688-701.

Das, P. K., 1950. The growth of cloud droplets by coalescence. Indian J. Met. Geophys. 1, 137.

Dingle, A. N., 1972. Rain Scavenging Studies, Progress Report No. 8, Contract No. AT(11-1)-1407 with U.S. Atomic Energy Commission. Dept. of Atmospheric and Oceanic Sciences, The University of Michigan, Ann Arbor. 103 + v pp.

Fankhauser, J.C., 1969. Convective processes resolved by a mesoscale rawinsonde network. J. Applied Meteor. 8, 778-98.

_____ , 1971. Thunderstorm-environment interactions determined from aircraft and radar observations. Mon. Wea. Rev., 99, 171-92.

Fitzgerald, J.W., 1973. Dependence of the supersaturation spectrum of CCN on aerosol size distribution and composition. J. Atmos. Sci., 28, 382-90.

Fonda, A. and H. Herne, 1957. The Aerodynamic Capture of Particles by Spheres. National Coal Board Min. Res. Est. Rep. No. 2068.

Hocking, L. M. and P. R. Jonas, 1970. The collision efficiency of small drops. Quart. J. Roy. Met. Soc. 96, 722-729.

Howell, W. E., 1949. The growth of cloud drops in uniformly cooled air. J. Meteor., 6, 134-149.

Junge, C. E., and E. McLaren, 1971. Relationship of cloud nuclei spectra to aerosol size distributions and composition. J. Atmos. Sci., 28, 382-90.

Kornfeld, P., 1970. Numerical solution for condensation of atmospheric vapor on soluble and insoluble nuclei. J. Atmos. Sci., 27, 256-64.

Lanczos, C., 1956. Applied Analysis. Prentice Hall, 539 pp.

Langmuir, I., 1948. The production of rain by a chain-reaction in cumulus clouds at temperatures above freezing. J. Met., 5, 172-192.

Langmuir, I. and K. B. Blodgett, 1946. A Mathematical Investigation of Water Droplet Trajectories. U.S. Army Air Force Tech. Rep. No. 5418.

Lilly, D. K., 1970. The numerical simulation of three-dimensional turbulence with two dimensions. In Numerical Solutions of Field Problems in Continuum Physics, G. Berkoff and R. S. Vargas, eds., SIAM-AMS Proc., Vol. II, 41-53. Providence, R.I., Amer. Mathematics Soc.

Low, R. D. G., 1969. A generalized equation for the solution effect in droplet growth. J. Atmos. Sci., 26, 608-11.

Ludlam, F. H.,1951. The production of showers by the coalescence of cloud droplets. Quart. J. Roy. Met. Soc. 77, 402-17.

Mason, B. J., 1957. The Physics of Clouds, London, Oxford Univ. Press, 481 pp.

_____, 1971. The Physics of Clouds, 2nd ed., London, Oxford Univ. Press, 671 pp.

Mason, B. J. and C. W. Chien, 1962. Cloud-droplet growth by condensation in cumulus. Quart. J. Roy. Meteor. Soc., 88, 136-42.

Mordy, W. A., 1959. Computations of the growth by condensation of a population of cloud droplets. Tellus, 11, 16-44.

Neiburger, M., and C. W. Chien, 1960. Computations of the growth of cloud droplets by condensation suing an electronic digital computer. Physics of Precipitation. Geophys. Monogr. No. 5., Washington, Amer. Geophys. Union, pp. 191-209.

Paluch, I., 1973. Private communication.

Scott, W. D. and P. V. Hobbs, 1967. The formation of sulfate in water droplets. J. Atmos. Sci., 24, 54-57.

Semonin, R. G., 1970. Study of Rainout of Radioactivity in Illinois, Ninth Progress Report, Contract No. AT(11-1)-1199 with U.S. Atomic Energy Commission. Illinois State Water Survey, Urbana, Illinois.

Shafrir, U. and M. Neiburger, 1963. Collision efficiencies of two spheres falling in a viscous medium. J. Geophys. Res. 68, 4141-4147.

Shafrir, U. and M. Neiburger, 1964. Collision Efficiencies of Two Spheres Falling in a Viscous Medium for Reynolds Numbers up to 19.2. University of California Occasional Papers, No. 1, Berkely, Univ. of Calif. Press, 140 + x pp.

Steiner, J. T., 1972. A Three-Dimensional Numerical Model of Atmospheric Convection. Report No. MW-73, Stormy Weather Group, McGill Univ., Montreal, Canada, July 1972. 103 pp.

Storebø, P. B., and A. N. Dingle, 1973. Removal of pollution by rain in a shallow air flow. Submitted to J. Atmos. Sci., April 1973.

Twomey, S., 1971. The composition of cloud nuclei. J. Atmos. Sci., 28, 377-381.

Warner, J., 1969a. The microstructure of cumulus cloud. Part I. J. Atmos. Sci., 26, 1049-59.

Weickmann, H. J. and H. J. aufm Kampe, 1953. Physical properties of cumulus clouds. J. Meteor., 10, 204-11.

Whittaker, E. and G. Robinson, 1924, Calculus of Observation. Blackie and Son, 395 pp.

SECTION II. LEAD (Pb) IN RAINFALL

Because of current interest in atmospheric transport of lead (Pb) and of the possibility that lead is less efficiently removed from the atmosphere than most other trace materials, we packaged a large number of rain samples and set them aside for lead analysis in conjunction with our sampling for tracer-In, airborne radioactivity and pollens, etc. These collections were made in the Illinois network in our 1969 and 1970 field seasons.

To support the analysis of these samples we obtained supplemental support from The University of Michigan through its Institute for Environmental Quality (IEQ). These funds were entirely used to support Mr. Joshi in the Pb-analysis, which incidentally involved a good deal of effort in improving the reproducibility of the anodic stripping voltammetry (ASV) technique for lead.

A brief report of this effort was prepared for IEQ. It is included here inasmuch as the support of this sub-project was also partly provided within our AEC contract.

A. Introduction and Objectives

As an adjunct study associated with our field research directed toward the study of rain scavenging by severe storms (reference 1, 2, 3), a large number of rain samples were acquired for the purpose of measuring the amount of lead (Pb) brought to earth by the rain. These samples are of two kinds. One kind is simply an aliquot taken from a much larger quantity (more than 1 kg) of rain collected by a passive sampler throughout the rainfall period. Such samplers were distributed broadly over an area of some 200 square miles near the central field station for the purpose of giving the areal distribution of deposition by rain of the various trace contaminants. The other kind of sample was taken as part of a series of samples through the course of each rainstorm at one or more of our "sequential sampling" stations for the purpose of revealing the temporal variations of the deposition rates.

We have analyzed samples of both kinds ostensibly to determine the amounts and rates of lead (Pb) deposition by rain in the vicinity of the field study (Central Illinois) in June, 1969 and 1970.

There are several interlaced objectives underlying this effort.

1. In view of the importance of Pb as a gasoline additive, it has become a significant atmospheric contaminant. In the period since about 1968, a public awareness of this fact and a demand to correct

it has arisen. Some measures to improve the situation had already been taken during 1969, and improvement may have become detectible by 1970. Our first objective is to observe whether and how much the rain deposition of lead has changed from 1969 to 1970 in the study area.

2. The analytical procedure for Pb is a special problem. To study Pb in air and rain requires the greatest sensitivity attainable, that is to say, measurements of nanogram (10^{-9} gm) amounts are required. The atomic absorption spectrometry (AAS) method, which is most widely used, is capable of measuring Pb in amounts down to a few tens of micrograms (10^{-5} gm). In short, AAS is about ten-thousand-fold too insensitive for effective atmospheric Pb analysis. The emerging technique of anodic stripping voltammetry (ASV), on the other hand, appears capable of giving the order of sensitivity and accuracy needed. The technique requires development and testing, but in broad terms, it is economical of time and equipment and holds a great deal of promise for Pb measurement in particular. This development, testing, and application of ASV to Pb analysis is a second objective of our effort.

Lest this be read as an unduly simple and inconsequential objective in itself, it is appropriate to note that the atmospheric budgets pertaining to Pb determine the extent to which it may accumulate in the air (its atmospheric lifetime) and the distances to which it may be transported. That it is not efficiently removed by natural processes is indicated by the large and increasing amounts

deposited in the ice caps of Greenland and Antarctica over the last half-century. These facts bear upon our knowledge of the human, animal and plant exposure to Pb and of the rates of increase (or decline) of the dosages experienced by these populations. Our immediate objective is,therefore, a step toward better knowledge of the atmospheric budget of lead (Pb).

B. The Samples and Results

A map of the sampling network is presented in Figure 1. The sequential sampling stations are designated M (the central field station), G-1, G-2, G-3 (three automatic sample-changing stations provided by Dr. Donald F. Gatz of Argonne National Laboratory).

Except for the sequential samples taken at the central station, all samples for ASV analysis were 100 ml aliquots taken from the general rain samples.

The best sets of samples were collected on six different rainfall days: 1 and 14 June 1969 and 1, 14, 15, and 20 June 1970. The number and types of samples are tabulated in Tables 1 and 2.

Table 1. Rain Samples for Pb Analysis, 1969

Date	Type of Sample	Number of Samples
1 June	Network	29
	Sequential	8
14 June	Network	58
	Sequential	21

Table 2. Rain Samples for Pb Analysis, 1970

Date	Type of Sample	Number of Samples
1 June	Network	123
	Sequential	76
14 June	Network	80
	Sequential	6
15 June	Network	93
	Sequential	143
20 June	Network	60
	Sequential	4

C. Analysis

Analysis of the rain water samples for lead content was done by means of anodic stripping voltammetry (ASV). Reviews of this technique have been published by Shain (1964) and Barendrecht (1966). The instrumental set up for the present work has been described by Harrison (1970).

The smallest lead concentration determined with reasonable reproducibility was 2 ng/ml. Because the atomic absorption method is much less sensitive, i.e., has a threshold of about 100 ng/ml, the method was checked by making repeated measurements for a number of samples. A statistical evaluation of the duplicated analyses was made and showed an average error of 20% at concentrations averaging 15 ng/ml. This is not unreasonable error for determination of such small amounts, but better reproducibility is desired, and apparently must depend upon obtaining more adequate control of the electrode surface properties.

D. Results

Rain water concentrations ranged from 60 to 354 ng/ml in the sequential samples taken during June 1969. In the network samples, the range was from 6 to 233 ng/ml for the same rains. The difference in the respective maximum concentrations is readily attributed to dilution of the network samples by the nature of the collection technique. The lower minimum in the network samples is attributed to remoteness from important lead sources.

In the 1970 series, the sequential samples ranged from 0 to 173 ng/ml, and the network samples from 0 to 114 ng/ml.

The fact that the concentrations were lower in the 1970 series than in the 1969 series is subject to adequate interpretation only by the consideration of a number of additional factors. For example, rainfall was markedly deficient in 1969, and excessive in 1970. This should yield a dilution effect in the latter series, consistent with the observations. In addition, the atmospheric circulation differences between the two seasons, and the differences in detail of the sampler positions with respect to the roads must be studied.

The deposition amounts (network samples) and rates (sequential samples) are found to be considerably higher in 1970 than in 1969 (Tables 3 and 4). This is attributed mainly to the higher rainfall amounts and rates, respectively, in 1970. The maximum deposition rate of 22, 300 $\mu g/m^2 hr$ corresponds to a rainfall rate of 129 mm/hr.

Table 3: 1969	1 June Net.	1 June Seq.	14 June Net.	14 June Seq.	Units
max. conc.	120	354	233	346	ng/ml
min. Conc.	18	60	6	60	ng/ml
max. dep. rate	257		571	1749	$\mu g/m^2hr$
min. dep. rate	50		17	60	$\mu g/m^2hr$

Table 4: 1970	1 June Net.	1 June Seq.	14 June Net.	14 June Seq.	15 June Net.	15 June Seq.	20 June Net.	20 June Seq.
max. conc.	74	88	114	158	60	173	33	80
min. conc.	0	--	1	16	--	18	2	36
max. depos. rate	1975*	4840	832*	3930	2100*	22300	234*	287
min. depos. rate		--	24*	10	--	298	11*	120

*Deposition in $\mu g/m^2$ NOT deposition rate

It is worthy of emphasis that this network is remote from large urban centers, the nearest being Springfield, Illinois, some 50 miles to the southwest. The sampling stations are rural mainly, although by necessity, they are adjacent to roads. We have begun a study which stratifies the data according to a road traffic index and to position of sampler (upwind, downwind, and distance) with respect to the adjacent roads, and these results will be reported elsewhere.

The values shown here are therefore representative of average rural conditions in central Illinois and perhaps the eastern half of the midwestern farm belt. They represent only the lead (Pb) deposited in association with rainfall, which is probably in particle sizes greater than 1 μm radius. If these amounts are pro-rated over the normal annual precipitation for the area, we find an annual lead deposition of the order of 20 mg/m^2.

E. References

Dingle, A. N., 1969. Rain Scavenging Studies, P.R. No. 6, Contract No. AT (11-1)-1407, U.S. Atomic Energy Commission, Dept. of Meteorology and Oceanography, The University of Michigan, Ann Arbor. 97 + x pp.

_____, 1970. Rain Scavenging Studies, P.R. No. 7., Contract No. AT (11-1)-1407, U.S. Atomic Energy Commission. Dept. of Meteorology and Oceanography, The University of Michigan, Ann Arbor. 62 + vii pp.

_____, 1972. Rain Scavenging Studies, P.R. No. 8., Contract No. AT (11-1)-1407, U.S. Atom ic Energy Commission. Dept. of Meteorology and Oceanography, The University of Michigan, Ann Arbor, 103 + v pp.

Shain, Irving, 1964, "Stripping Analysis", Treatise on Analytical Chemistry, Volume 4, Wiley, Interscience, New York, pp. 2533.

Barendrecht, E., 1966, "Stripping Voltammetry", Electroanalytical Chemistry, Volume 2, (ed., A.J. Bard), Marcel & Dekker, pp 53ff.

Harrison, P. R., 1970. Area-wide distribution of lead, copper, cadmium, and bismuth in atmospheric particles in Chicago and northwest Indiana, in multi-sample application and anodic stripping voltammetry, Ph.D. Thesis, The University of Michigan, Ann Arbor.

SECTION III

PAPERS SUBMITTED FOR PUBLICATION

A. An Analysis of In-Cloud Scavenging

A. Nelson Dingle

Yean Lee

Department of Atmospheric & Oceanic Science, The University of Michigan
Ann Arbor 48104

ABSTRACT

The fate of airborne contaminants that enter a cloud with an overriding rain, independently generated, is considered by means of three differential equations which express the overall mass conservation of contaminant. The model incorporates the well-known physical processes, diffusive attachment, impact collection and accretion, and includes consideration of particle and cloud droplet size spectra. The rainout ratio and rainout efficiency are evaluated on the basis of the theoretical results, and the general expressions for different cloud conditions are proposed.

1. Introduction

The scavenging of contaminant by precipitation is frequently treated in two parts, i.e., that occurring below cloud (washout) and that within cloud (rainout). For the below-cloud case, the theoretical predictions are available. (Zimin, 1964; Engelmann, 1968; Slinn and Hales, 1971). The situation for the in-cloud case is less satisfactory. Beginning with the paper by Greenfield (1957) a number of papers have appeared which treat various parts of the problem (e.g., Goldsmith and Delafield, 1963; Hicks, 1966, Vittori and Prodi, 1967; Slinn and Hales, 1971; Davis, 1972), but no comprehensive treatment has so far appeared. The purpose of the present study is to put forward a simplified model of in-cloud scavenging which incorporates the well-known physical processes and includes consideration of particle and cloud droplet size spectra.

2. The Model

In the present model, the cloud is envisaged as an assembly of droplets mixed with a particulate contaminant some of which is free-floating in the cloud air and some of which is attached to the droplets. Overriding rain, independently generated, removes contaminant particles of both classes.

The temporal variation of the contaminant concentration in each category is expressed by means of an ordinary differential equation as follows

$$\frac{dN_a}{dt} = -(\alpha + \beta + \gamma) N_a \tag{1}$$

$$\frac{dN_c}{dt} = \alpha N_a - \lambda N_c \tag{2}$$

$$\frac{dN_r}{dt} = \lambda N_c + (\beta + \gamma) N_a \tag{3}$$

where

N_a = number density of contaminant particles in the cloud air, cm^{-3}

N_c = number density of contaminant particles attached to cloud droplets, cm^{-3}

N_r = number density of contaminant particles removed by raindrops, cm^{-3}

α = diffusive attachment rate between particles and droplets, sec^{-1}

β = diffusive attachment rate between particles and raindrops, sec^{-1}

γ = impact collection rate for particles by raindrops, sec^{-1}

λ = rate of accretion of droplets by raindrops, sec^{-1}

and the system conserves contaminant mass.

3. Analysis

Obviously as long as α, β, γ, and λ are considered constants, the equations can be integrated analytically in time. If the contaminant is allowed to mix with the cloud for a time, t_c, before precipitation begins, then the air concentration can be written directly:

$$N_a\ (t_c) = N_a\ (0)\ e^{-\alpha t_c} \tag{4}$$

where $N_a\ (0)$ is the initial particle concentration in the cloud air. The number of particles associated with the droplets prior to the rain is

$$N_c\ (t_c) = N_c\ (0) + N_a\ (0)\ (1 - e^{-\alpha t_c}) \tag{5}$$

where $N_c\ (0)$ is the number density of the particles that serve as condensation nuclei as the cloud is formed.

After the onset of rain, the number density of contaminant particles remaining in the cloud air at time t, measured from the onset of rain, becomes

$$N_a\ (t) = N_a\ (0)\ e^{-\alpha t_c}\ e^{-(\alpha + \beta + \gamma)t} \tag{6}$$

The number density of contaminant particles associated with the remaining cloud droplets is then

$$N_c\ (t) = [N_c\ (0) + N_a\ (0)(1 - e^{-\alpha t_c})]\ e^{-\lambda t} +$$

$$\frac{\alpha N_a\ (0)\ e^{-\alpha t_c}}{\lambda - (\alpha + \beta + \gamma)}\ (e^{-(\alpha + \beta + \gamma)t} - e^{-\lambda t}) \tag{7}$$

and the number of pollution particles per unit volume removed by raindrops can be written as

$$N_r(t) = \{N_c(0) + N_a(0)\}\ (1 - e^{-\lambda t}) +$$

$$\frac{N_a(0)\, e^{-\alpha t_c}}{\lambda - (\alpha + \beta + \gamma)} \{e^{-\lambda t} - e^{-(\alpha + \beta + \gamma)t}\} \{\lambda - (\beta + \gamma)\} \quad (8)$$

Evaluation of Parameters. The rate constants must be evaluated in terms of the respective physical processes.

a) Diffusive attachment. The particles become attached to the droplets by Brownian and turbulent diffusion, each of which contributes to the value of α. If α_B is the rate of attachment contributed by Brownian diffusion, then

$$\alpha_B = \frac{kT}{3\eta} \left(\frac{1 + a\ell/r_p}{r_p} + \frac{1 + a\ell/r}{r}\right) (r_p + r)\, M_c \quad (9)$$

where

r_p is the particle radius, and r is the droplet radius,

a is the Cunningham correction factor (=0.9),

ℓ is the mean free path of air molecules taken as 10^{-5} cm,

M_c is the number density of cloud droplets, cm^{-3}

k is the Boltzmann's constant, T is the absolute temperature, and η is the air viscosity.

For the contribution, α_T, of air turbulence to the attachment rate, we write

$$\alpha_T = 14.1\ (r_p + r)^3\ \left(\frac{\varepsilon}{\nu}\right)^{\frac{1}{2}} M_c \qquad (10)$$

following Levich (1962). Here ε is the rate of energy dissipation, ν is the kinematic viscosity. The quantity, ε, is dependent upon the nature of the cloud considered. Ackerman (1968)gives a value of 6.4 $cm^2\ sec^{-3}$ as the average for stratiform cloud. We consider the turbulent and Brownian contributions to be additive, hence

$$\alpha = \alpha_B + \alpha_T \qquad (11)$$

To complete the evaluation of the diffusive attachment rate, α, the size spectra of the contaminant particles and the cloud droplets are required. For the present work, we adopt the formulation of Khrgian and Mazin (1961):

$$n\ (r) = a\ r^2\ e^{-br} \qquad (12)$$

where n (r) is the number of droplets per unit volume in the radius interval between r and r + dr, and

$a = (1.45\ \bar{r}^{-6})Q$

$b = 3\ \bar{r}^{-1}$

Q is the liquid water content, gm cm^{-3}

and $\bar{r} = \frac{1}{N} \int_o^\infty r\ n\ (r)\ dr$ is the average radius.

The particle size spectrum is chosen to be log-normal, and is specified in terms of the geometric modal radius, r_m, and the geometric standard deviation, σ. For the present model, $r_m = 10^{-5}$cm and $\sigma = 2.5$. Therefore

$$N_p = A \exp\left[-0.5 \left(\ln \frac{r_p}{r_m}\right)^2 (\ln \sigma)^{-2}\right] \qquad (13)$$

where N_p is the number of particles per unit volume in the radius interval between r_p and $r_p + dr_p$. For the computations, the size spectrum is composed of 30 classes at intervals of

$r_{n+1} = 2^{\frac{1}{3}} r_n$, and r_o is chosen at 10^{-6} cm.

The same treatment is used to evaluate the diffusive attachment between particles and raindrops. Here, the Marshall-Palmer (1948) raindrop-size formulation is used.

b) Impact collection. The impact collection rate is

$$\gamma = \Sigma \left[\pi R^2 E(r,R) (V_R - V_r) N_R \Delta R\right] \qquad (14)$$

where V_R is the terminal velocity of raindrops of radius R, V_r is the terminal velocity of particles of radius r, E(R,r) represents the collision efficiency, and $N_R \Delta R$ is the number of raindrops perunit volume in the size range R to R + ΔR. Values of E are derived from the table compiled by Mason (1971) after graphic smoothing (Storebø and Dingle, 1973).

c) Accretion. The removal of cloud droplets by rain is given by equation (14) when R denotes the raindrop radius, r the cloud droplet radius, and when λ is substituted for γ.

4. Results

Four cases have been selected to bring out the scavenging effects of various parameters of the model. In the computations, the cloud spectrum and size distribution of pollution are assumed to be time-independent, and the term $N_c(0)$ of Equation (5), (7) and (8) is not accounted for.

a) Case I: Steady state cloud: cloud water replenished at rate exactly equal to rate of removal of cloud water by falling rain. Removal of pollution particles by a) Brownian and turbulent attachment to cloud droplets and falling rain, and b) removal of cloud water with attached pollution by falling rain. Results for this case are shown in Fig. 1 and Fig. 2. The pollution mass (%) remaining in the cloud region after time t at various rainfall rates is given in Fig. 1b.

As it is found, the impact-collection of pollution particles by the falling raindrops is not an effective means of removing them from the air, since particles smaller than 2 μm radius are not captured by raindrops, (i.e. $E(R,r) \to 0$) and particles greater than 2μ radius have a very low concentration. As shown in Fig. 1a, the amount of contaminant attached to cloud droplets is initially zero. It increases, reaches a maximum after a time which is dependent upon the relative magnitudes of attachment rate and scavenging rate, and then decreases gradually. Fig. 2a shows the trend of the integral mass (%) removed from the cloud at various rainfall rates. It is found that about 29% of the contaminant is scavenged by a rainfall of intensity 10 mm/hr in four hours. The removal rate for ten-minute intervals in % per hour is shown in Fig. 2b. The heavier the precipitation, the earlier the maximum removal rate occurs.

b) Case II: Similar to Case I except that the cloud is not replenished. In this case, the concentration of cloud droplets decreases

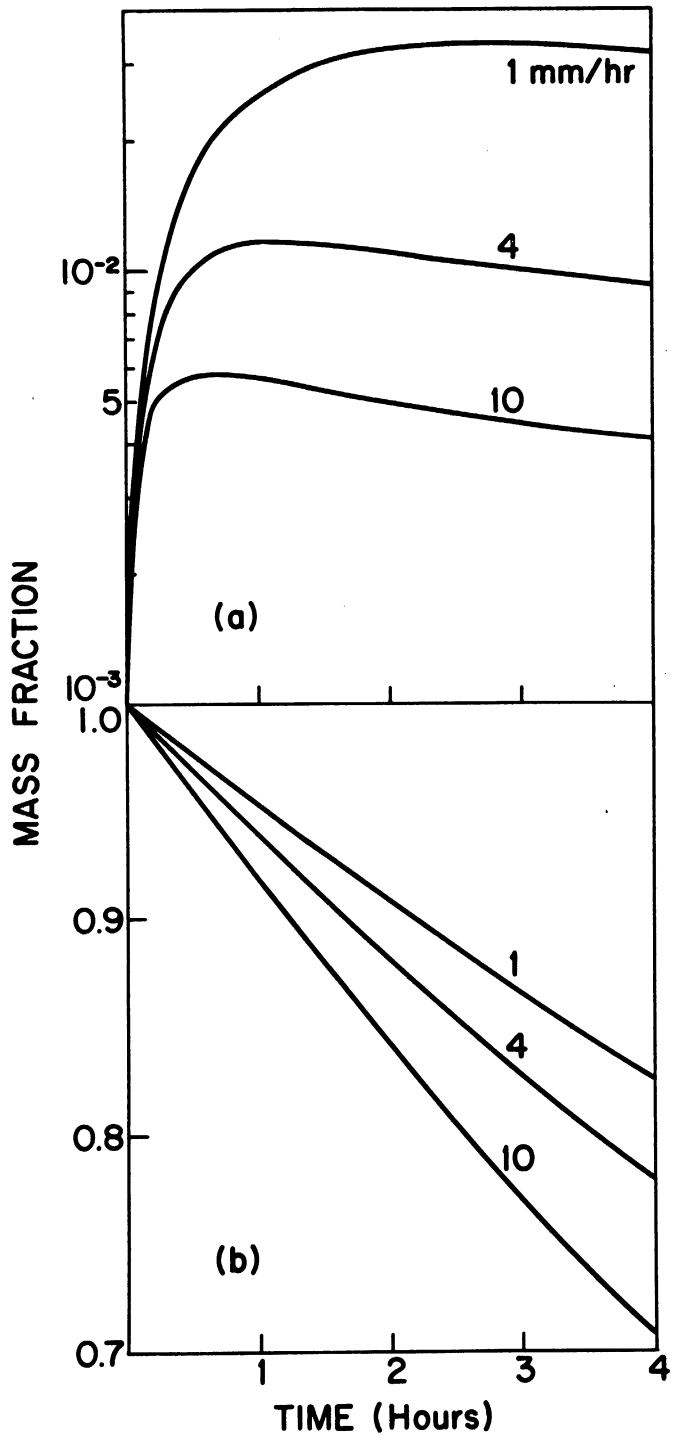

Fig. 1. Case I. Cloud water constant (replenished). (a) fraction of mass attached to cloud droplets and (b) fraction of mass remaining in cloud air as a function of time.

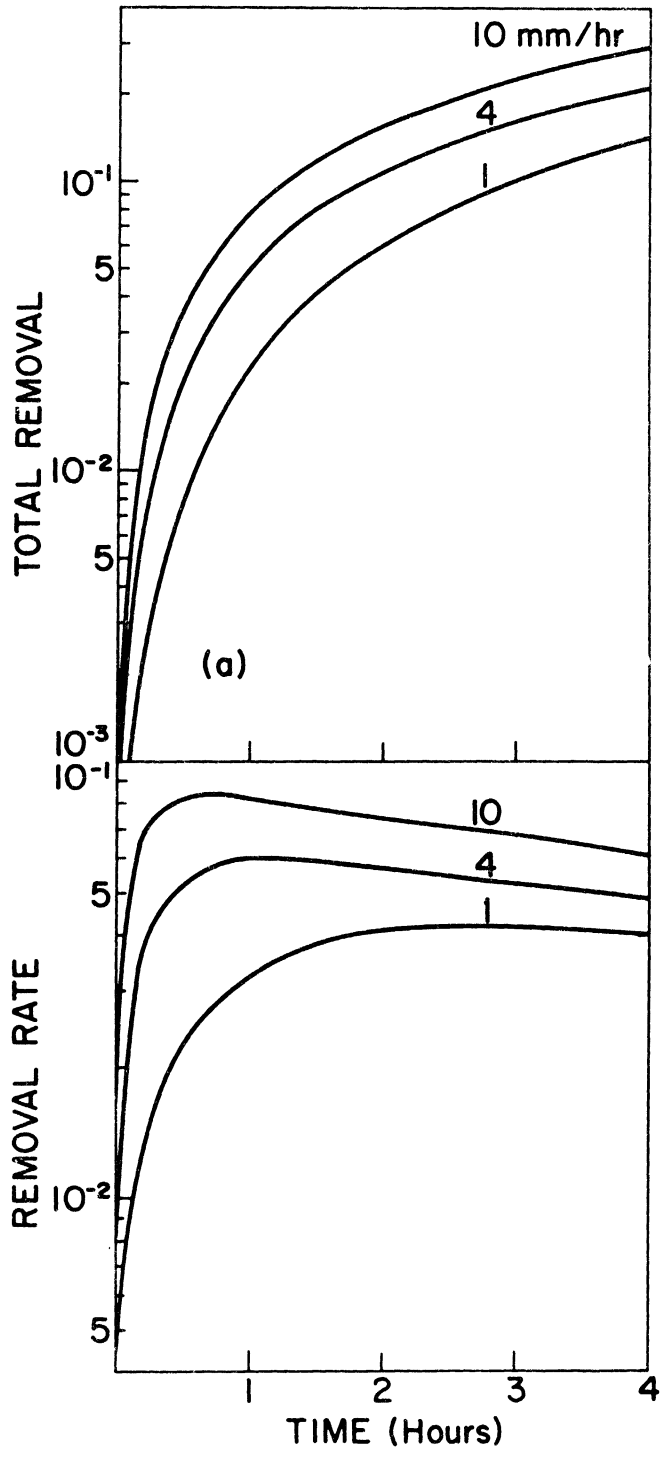

Fig. 2. Case I. Cloud water constant (replenished). (a) Integral fraction of mass removed by rainfall and (b) removal rate as a function of time

with time. This decrease in drop concentration in turn leads to a lower rate of attachment of particles to cloud droplets. Thus, the parameter α can no longer be treated as a constant for the whole period of precipitation. To simplify our computations, we assume that the parameter α remains constant for a short time interval and is adjusted for each time step. The time step is mainly determined by the amount of water removed from the cloud. In our computation, it is shown that the weighted accretion rate, λ, ranges from $10^{-4}(sec^{-1})$ to $10^{-3}(sec^{-1})$. For rainfall rates less than 4 mm/hr, the cloud water removed every two minutes does not significantly change the cloud droplet concentration. Therefore, the attachment rate may be considered constant for this time interval. For rainfall rates greater than 4 mm/hr, the water content remaining in the cloud is redistributed after every minute and α is readjusted accordingly.

Fig. 3 and Fig. 4 show the results for case II. The trend of pollution remaining in the air is similar to that in Fig. 1b. The major difference between Fig. 1b and Fig. 3b is the relatively small amount of material scavenged in the latter. The obvious reason for this is that cloud water is decreased. The maximum removal rates occur at an earlier stage in case II than in case I. Also the diffusive attachment processes lead to an earlier maximum of pollution mass acquired by cloud droplets in case II than in case I (Fig. 3a).

c) Cases III & IV: Case III is similar to case I except that a two-hour period of residence of pollution particles in the cloud is allowed prior to the onset of rain. Case IV is similar to case III except that the cloud is non-steady as in case II. In these

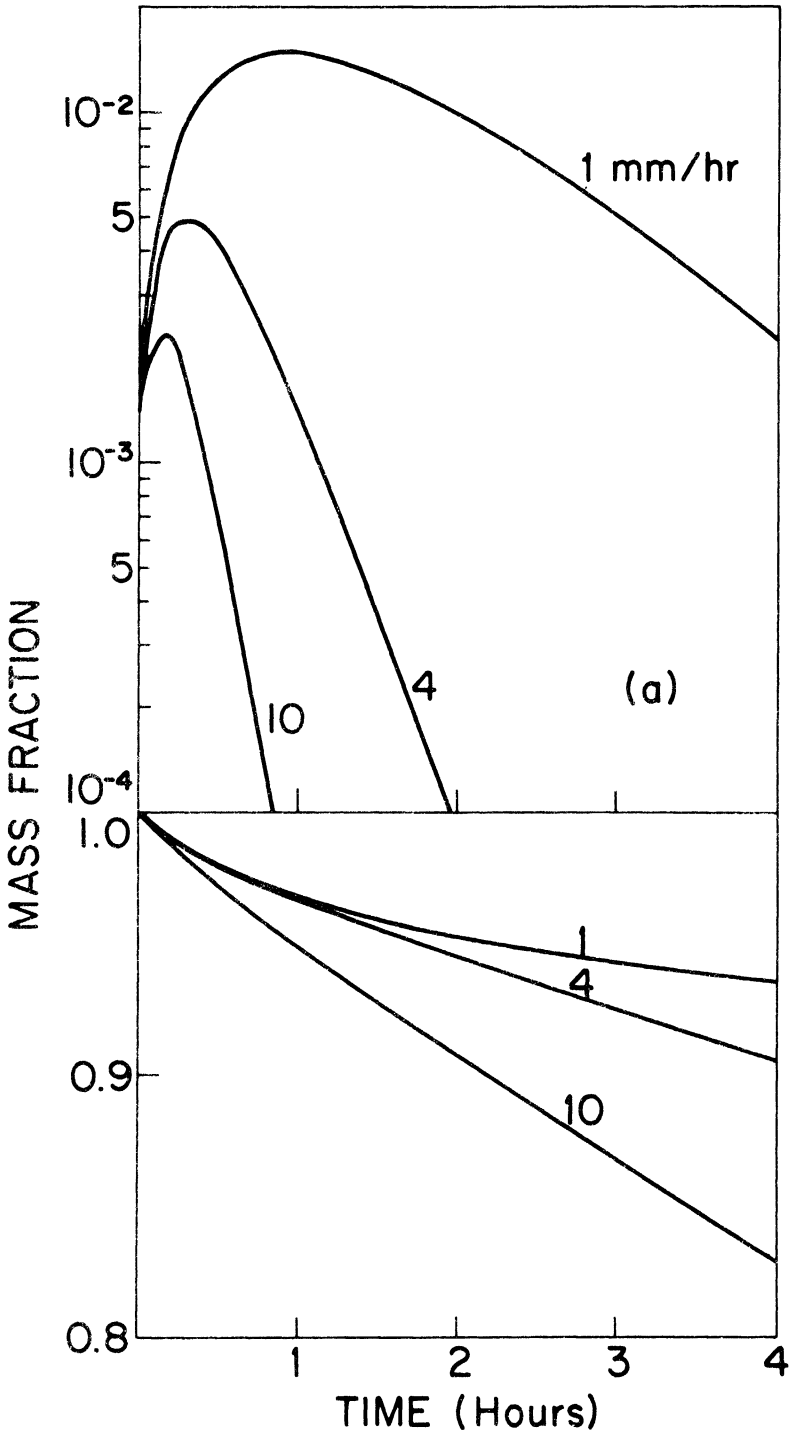

Fig. 3. Case II. Decreasing cloud water. (a) Fraction of mass attached to cloud droplets and (b) fraction of mass remaining in cloud air as a function of time.

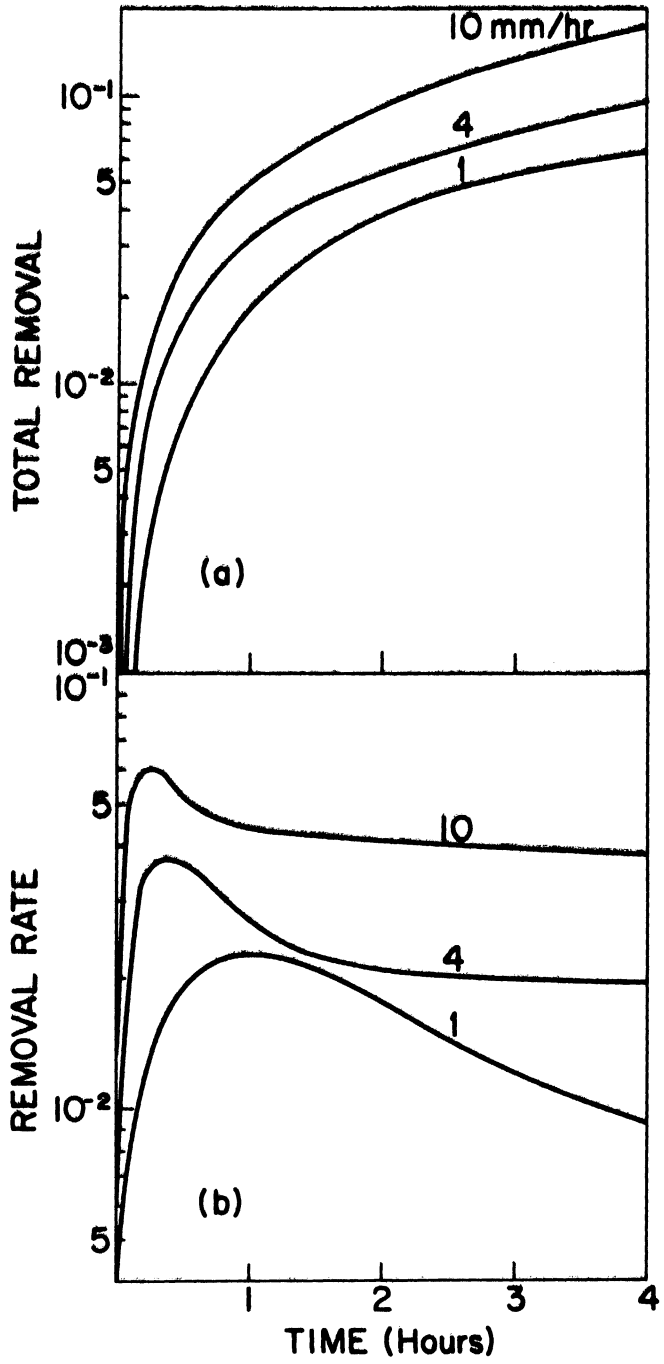

Fig. 4. Case II. Decreasing cloud water. (a) Integral fraction of mass removed by rainfall and (b) removal rate as a function of time.

cases, the in-cloud mixing time t_c is two hours, and rain falls through the polluted cloud for another two hours. Results for these cases are shown in Figs. 5,6 and Figs. 7, 8. What is effectively demonstrated by these modeled cases is the increased removal of pollution mass where preliminary mixing is allowed. For example, in case III (Fig. 5b), after two hours during which the rainfall rate is 10 mm/hr, the air contains 77% polluting materials. In contrast to this is case I (Fig 1b) where approximately 84% polluting materials still reside in the air. One important difference brought out by cases III and IV is that the contaminant mass fraction attached to cloud droplets has a completely different pattern from case I or case II. The same feature appears in the removal rate of pollution mass. This is due to the fact that by the time rain starts, the cloud droplets have already been acquiring contamination for two hours.

d) Rainout efficiencies. For each case, a semi-empirical relationship between the mass fraction remaining in cloud air, the rainfall intensity and the precipitation time can be derived from the computational results. The respective equations are:

$$F_1 = 1 - (.044 + .0042\ I)t^{0.90} \qquad (15a)$$

(steady state, case I)

$$F_2 = 1 - (.028 + .0017\ I^{1.35})t^{0.68} \qquad (15b)$$

(non-steady state, case II)

$$F_3 = 1. - [(.044 + .0042I)t^{0.9} + .08] \qquad (15c)$$

(steady state, case III)

$$F_4 = 1. - [(.028 + .0017\ I^{1.35})t^{0.68} + .08] \qquad (15d)$$

(non-steady state, case IV)

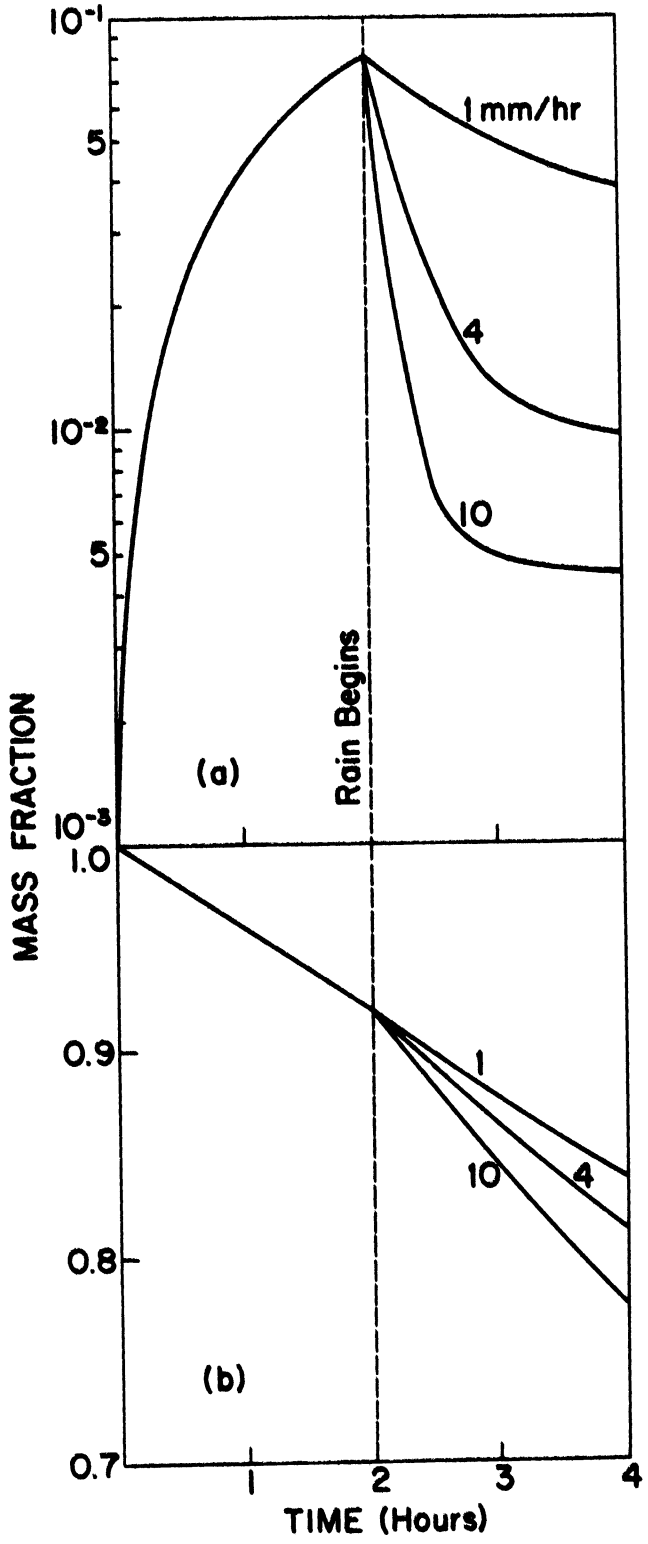

Fig. 5. Case III. Cloud water constant (replenished). Rain begins at time t = 2 hr. (a) fraction of mass attached to cloud droplets and (b) fraction of mass remaining in cloud air as a function of time.

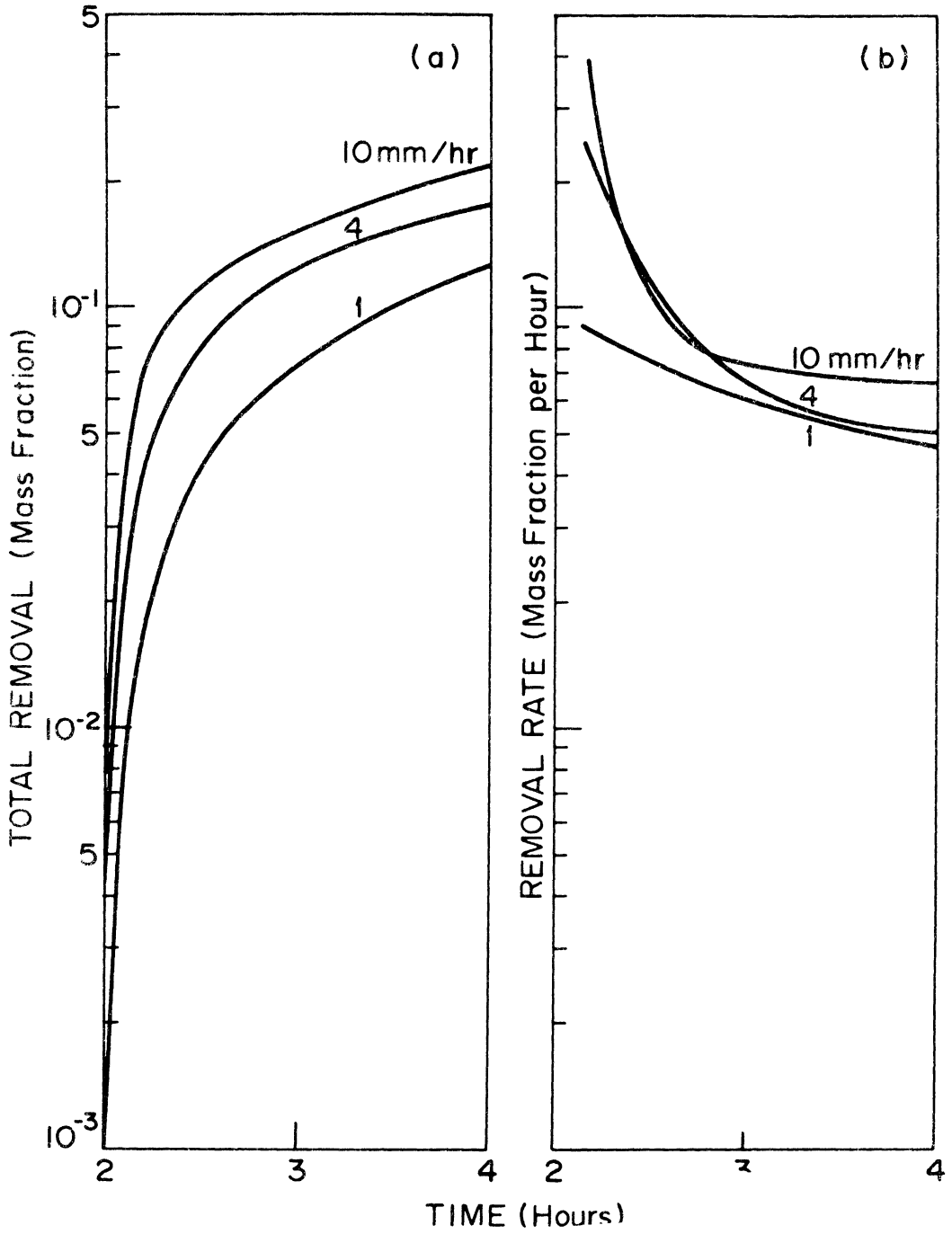

Fig. 6. Case III. Cloud water constant (replenished). Rain begins at time t = 2 hr. (see Fig. 5) (a) Integral fraction of mass removed by rainfall and (b) removal rate as a function of time.

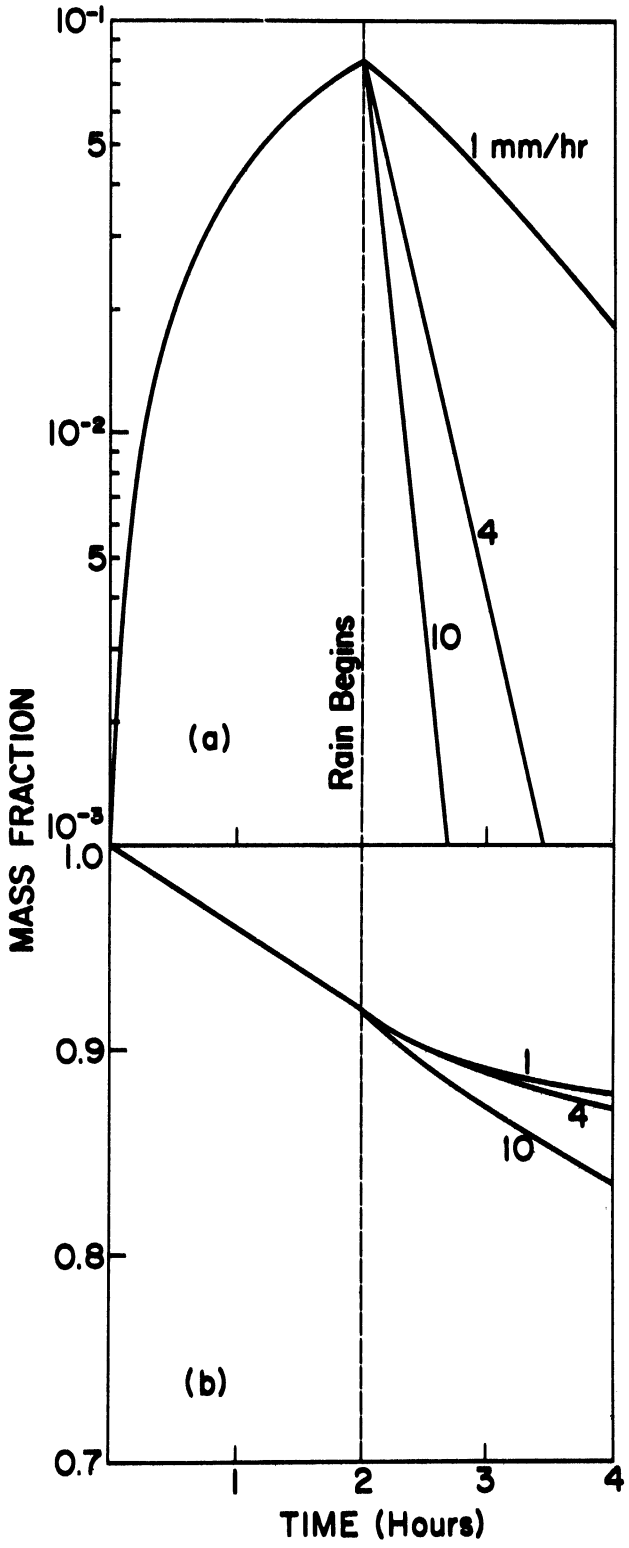

Fig. 7. Case IV. Decreasing cloud water. Rain begins at time t = 2 hr. (a) Fraction of mass attached to cloud droplets and (b) fraction of mass remaining in cloud air as a function of time.

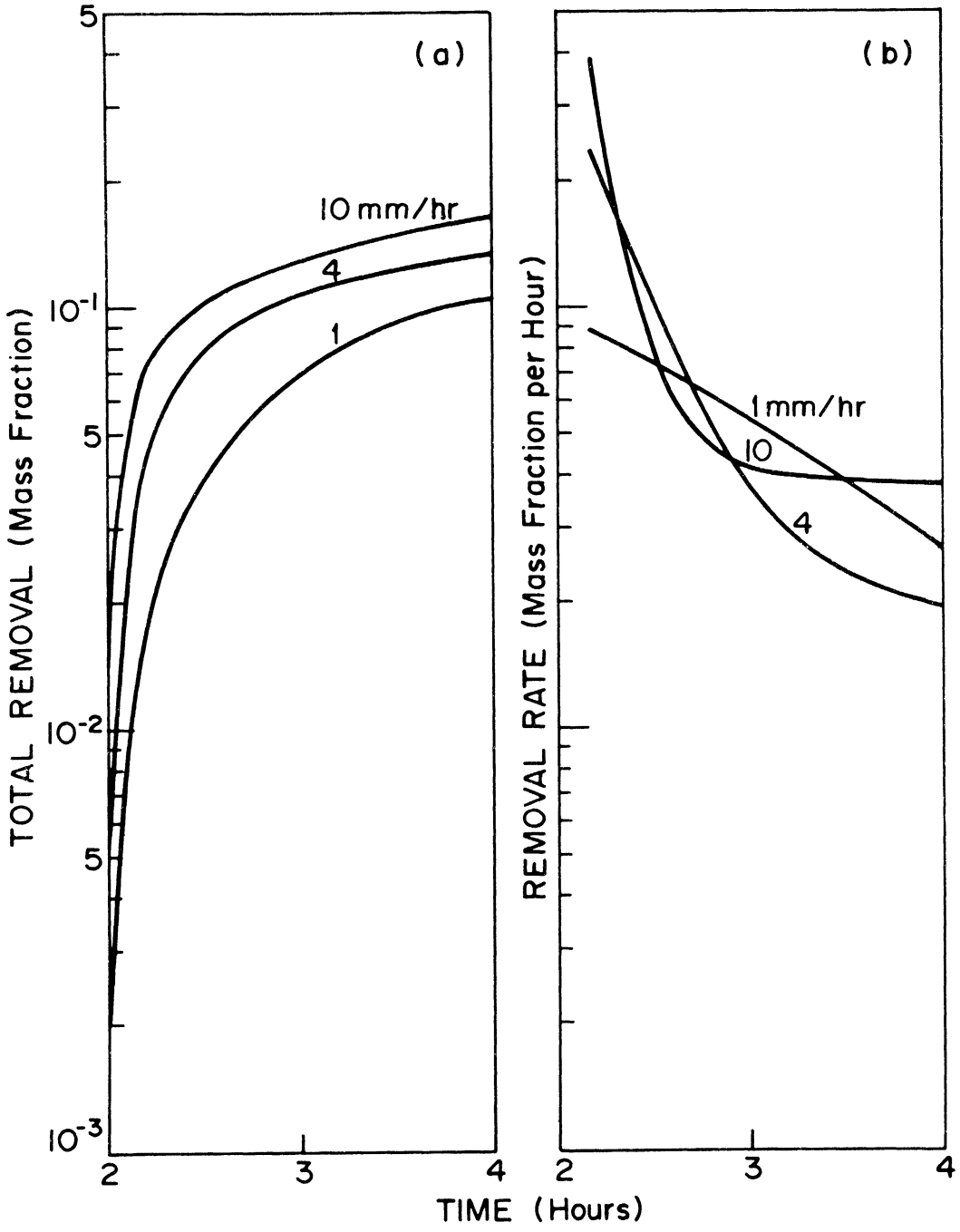

Fig. 8. Case IV. Decreasing cloud water. Rain begins at time t = 2 hr. (see Fig. 7) (a) Integral fraction of mass removed by rainfall and (b) removal rate as a function of time.

where F is the mass fraction remaining in cloud air, I rainfall intensity (mm/hr), t precipitation time (hr). With these equations, the rainout efficiency (Engelmann, 1968) for each case can be expressed as

$$E_1 = 1 - F_1 = (.044 + .0042\ I)\ t^{0.90} \tag{16a}$$

$$E_2 = 1 - F_2 = (.028 + .0017\ I^{1.35})\ t^{0.68} \tag{16b}$$

$$E_3 = 1 - F_3 = (.044 + .0042\ I)\ t^{0.90} + .08 \tag{16c}$$

$$E_4 = 1 - F_4 = (.028 + .0017\ I^{1.35})\ t^{0.68} + .08 \tag{16d}$$

Junge (1963) introduces the equation

$$K = \chi_o\ E\ \frac{\rho}{Q} \tag{17}$$

where K is the aerosolper volume of cloud water, χ_o aerosol per volume of unwashed air, ρ density of water, Q liquid water content. Engelmann (1971) defines a "washout ratio" in terms of K/χ_o. In the present context, the term "rainout ratio" appears more appropriate.

Introducing E_i into Eq. (17), we have

$$\frac{K}{\chi_o} = E_i \frac{\rho}{Q} \tag{18}$$

This shows that the rainout ratio varies directly with precipitation rate and duration of rainfall. With reasonable value of Q, here $Q = 3.0 \times 10^{-7}$ gm/cm^3, the rainout efficiency and the rainout ratios can be determined. Fig. 9 and Fig. 10 show these results which compare favorably with experimental observations (see Table 1.)

Referring to Fig. 9 we can see that for various rainfall intensities and precipitation times, the rainout efficiency is in the range of 0.03 - 0.3. In view of the semi-empirical expressions

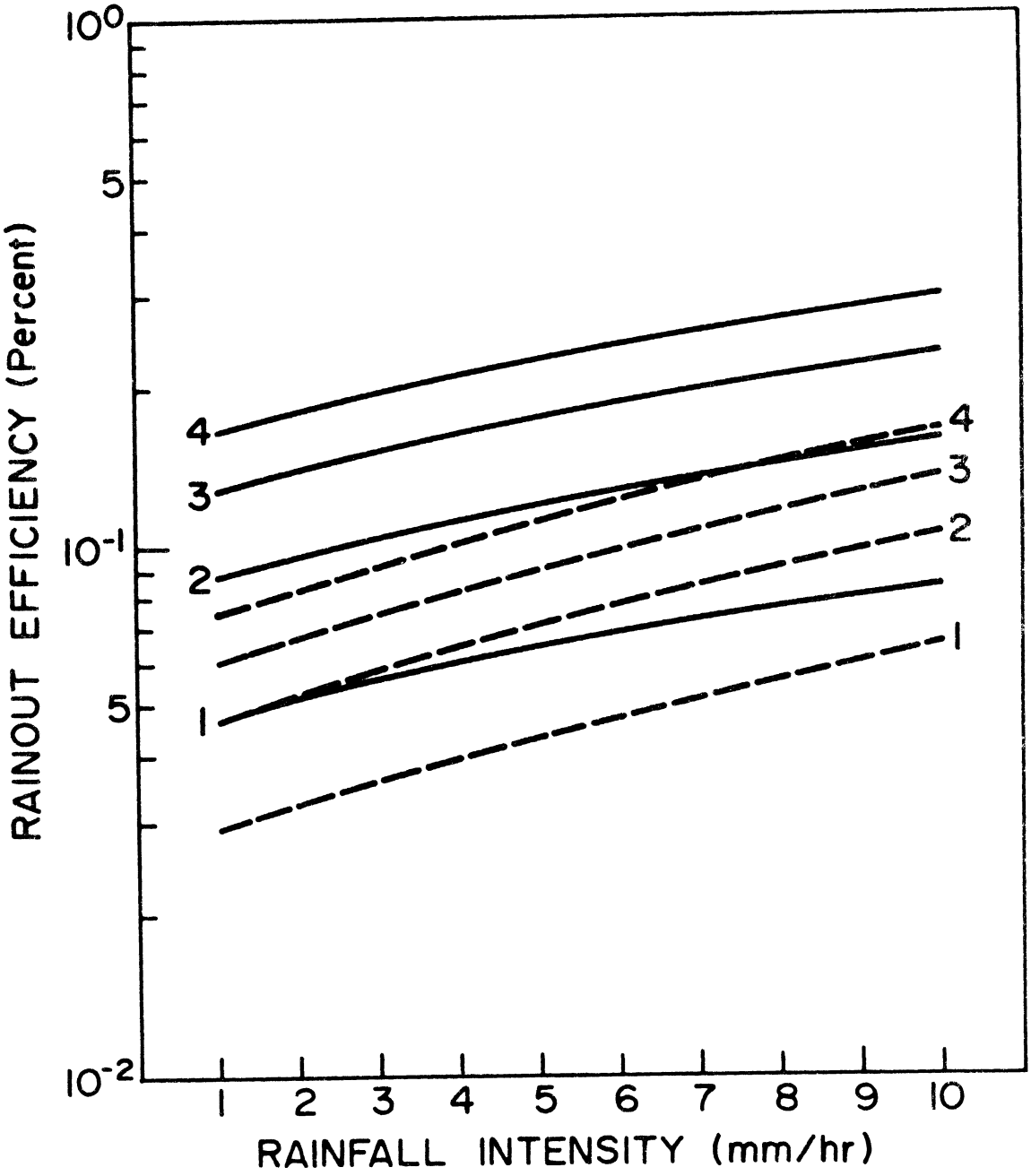

Fig. 9. Rainout efficiency vs rainfall intensity. Case I (solid) and Case II (dashed). Precipitation time in hours is indicated by the numbers.

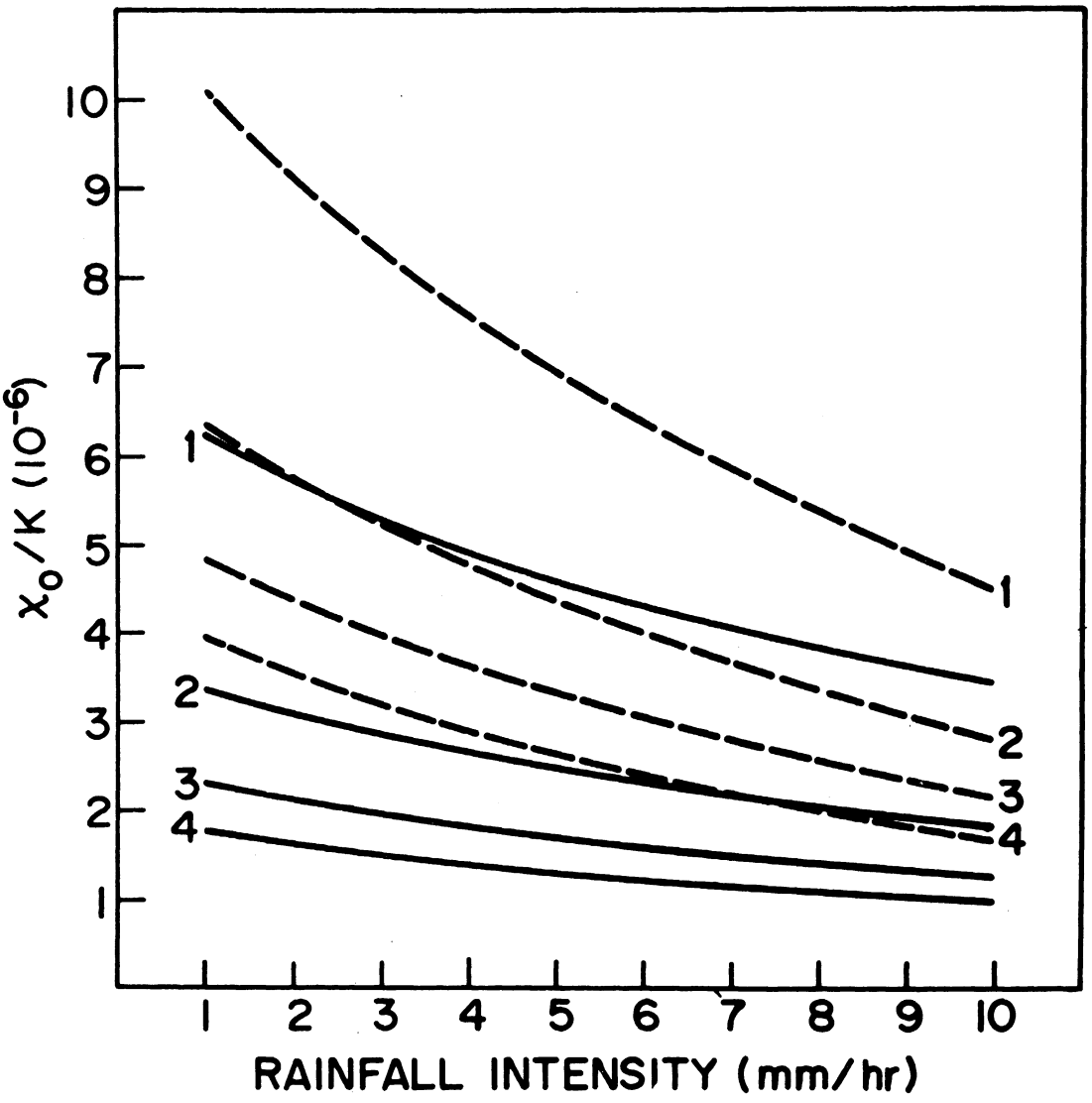

Fig. 10. X_o/K vs rainfall intensity. Case I (solid) and case II (dashed). Precipitation time in hours is indicated by the numbers.

Table 1: SELECTED MEASUREMENTS OF SURFACE AIR TO PRECIPITATION ACTIVITY RATIOS AND VALUES OF CLOUD-WATER CONCENTRATION CHOSEN TO PRODUCE RAINOUT EFFICIENCIES BETWEEN 0.5 AND 1.0.

DATA SOURCE	χ_o/K	K/χ_o	Q/ρ	E or ΨT
Small*(Norway)				
October 1956	0.25×10^{-6}	4.0×10^{6}	0.25×10^{-6}	1.0
September 1959	2.06	0.47	2.0	0.95
Average (3 year)	0.9	1.1	0.9	1.0
Hinzpeter (Germany)				
Rain, mm/day				
0.1	0.8	1.25	0.5	0.62
1.0	1.4	0.71	1.0	0.71
10.0	2.5	0.40	2.0	0.8
Snow, mm/day (water equivalent)				
0.15	0.9	1.1	0.5	0.55
1.0	1.6	0.62	1.0	0.62
10.0	3.4	0.29	2.0	0.59

* S.H. Small, 1960 (after Engelmann, 1968)

Hinzpeter, 1958

deduced for different cases, we may suggest a more general expression for the in-cloud rainout efficiency as

$$E = (E_d + a_o I^{a_1}) t^{a_2} + E_n \qquad (19)$$

where E_n is the fraction of pollutant serving as condensation nuclei, a_o, a_1 and a_2 are constants, E_d can be considered as the fraction of pollutant attached to precipitation elements due to diffusive processes, the meteorological parameters I and t can be well determined. If one assumes $E_d = 0.036$, $a_o = .003$, $a_1 = 1.2$, $a_2 = 0.8$, $I = 4$ mm/hr, $t = 4$ hours, and $E_n = 0.5$, we obtain a value of $E = 0.66$ which is in the range of values suggested by Junge (1963) and by Engelmann (1971).

5. Conclusion

The parameters introduced into this model are evaluated in accordance with well known physical processes and take into account particle and droplet size spectra. In the previous studies, Greenfield (1957) proposed the theory of scavenging of contaminant on the basis of monodispersed particles and droplets. Makhon'ko (1967) and Davis (1972) have deduced the order of magnitude of these parameters (α, λ) from the ground experimental data. Within the limits of our model, the order of magnitude, shown by these computations, is 10^{-5} to 10^{-4} for α, 10^{-6} to 10^{-5} for β, and 10^{-4} to 10^{-3} sec^{-1} for λ, which compare favorably with the experimental results. The value of γ is found to be negligible as noted above. The case of constant cloud water (cases I & III) may be considered as an upper limit for the fraction scavenged, while on the other hand, the case of reducing cloud water (cases II & IV) may be considered as a lower limit.

The removal rate pattern is closely related to the time of residence of the contaminant in the cloud region before precipitation starts and also to the rainfall rate. The method and the results provide new insights into the influence of such parameters as size spectrum, cloud water content, rainfall rate, and attachment mechanism in the scavenging effect.

The parameters involved in the general expression Eq. (19) can be varied over some limits in order to determine the effects of processes being parameterized. The estimates of E show that the nucleation process itself is the most efficient attachment mechanism

but that diffusive processes are also important. With the measurements of rainfall intensity and precipitation time, the rainout efficiency can be well estimated.

Acknowledgement: This research has been supported by the Earth Sciences Branch, Division of Biomedical and Environmental Research, U.S. Atomic Energy Commission under Contract No. AT(11-1)-1407.

6. References

1. Ackerman, B., 1968: The rate of dissipation of turbulent energy in cloudy air. Proceedings of the International Conference on Cloud Physics, 564-567.
2. Borovikov, A.M., and A. Kh. Khrgian, 1961: Cloud Physics. (available from the Clearinghouse for Federal Scientific and Technical Information, Springfield, VA., OTS-63-11141).
3. Davis, W.E., 1972: A model for in-cloud scavenging of Cosmogenic Radionuclides, J. Geophys. Res., 77. 2159-2165.
4. Engelmann, R.J., 1968: Meteorology and atomic energy. U.S. Atomic Energy Commission. TID-24190. 208-221.
   1971: Scavenging prediction using ratios of concentrations in air and precipitation. J. Appl. Meteor. 10, 493-497.
5. Goldsmith, P., and H.J. Delafield and L.C. Cox, 1963: The role of diffusiophoresis in the scavenging of radioactive particles from the atmosphere, Quart. J. Roy. Met. Soc., 89, 43-61.
6. Greenfield, S.M. 1957: Rain scavenging of radioactive particle matter from the atmosphere. J. Meteor. 14, 115-125.
7. Hicks, B.B., 1966: Nucleation and wet removal of fallout, J. Appl. Meteor., 5, 169-174.
8. Hinzpeter, M., 1958: The influence of meteorological parameters on the propagation of radioactive fission products in the biosphere. Proc. Second Intern. Conf. Peaceful Uses of Atomic Energy, Vol. 18, Geneva, United Nations, 284-290.

9. Levich, V.G., 1962: Physico-chemical Hydrodynamics. Prentice-Hall, Inc., Englewood Cliffs, N.J.

10. Makhon'ko, K.P., 1967: Simplified theoretical notion of contaminant removal by precipitation from the atmosphere. Tellus, 19, 467-476.

11. Marshall, J.S. and W.M. Palmer, 1948: The distribution of raindrops with size. J. Meteor., 5, 165-166.

12. Mason, B.J. 1971: The physics of clouds, Clarendon Press, Oxford. 671 pp.

13. Slinn, W.G.N., and J.M. Hales, 1971: A re-evaluation of the role of thermophoresis as a mechanism of in- and below-cloud scavenging. J. Atmos. Sci, 28, 1465-1471.

14. Small, S.H., 1960: Wet and dry deposition of fallout materials at Kjeller. Tellus, 12, 308-314.

15. Storebø, P.B., and A.N. Dingle, 1973, Removal of pollution by rain in a shallow air flow (submitted for publication in the Journal of the Atmospheric Sciences).

16. Vittori, D.A., and V. Prodi, 1967: Scavenging of atmospheric particles by ice crystals, J. Atmos. Sci., 24, 533-538.

17. Zimin, A.G., 1962: Mechanisms of capture and precipitation of atmospheric contaminants by clouds and precipitation. AEC-Tr-6128, 1964.

B. Ammonium Sulfate Crystallization in Andersen Cascade Impactor Samples

by

A. Nelson Dingle

and

Bhanuprasad M. Joshi

Department of Atmospheric and Oceanic Sciences
The University of Michigan
Ann Arbor, 48104

ABSTRACT

Meteorologists are accumstomed to the atmospheric phase changes of water. It is observed that phase changes ending with crystallization and crystal growth of $(NH_4)_2SO_4$ take place in Andersen Samplers used to collect size-stratified samples of airborne particles. It is not at this point clear whether pre-formed $(NH_4)_2SO_4$ crystals of small size are involved, although this is likely, but the cascade impaction processes evidently play a role in generating large $(NH_4)_2SO_4$ crystals on the last few stages of these samplers.

1. Introduction

Ammonium sulfate is one of the important constituents of continental aerosols [Junge (1954), Eggleton (1964)]. Garland (1969) has studied the effect of ammonium sulfate particles on visibility. Healy et al (1970) have reported the formation of ammonium sulfate and removal of ammonia from the troposphere. The present study deals with the formation and growth of ammonium sulfate crystals during sampling with an Andersen sampler. These cascade type impactors have been widely used for field collection of airborne particles in size-stratified samples. By means of various analytical techniques including atomic absorption [Nifong (1970)], neutron activation analysis [Rahn (1971)] and anodic stripping voltametry [Harrison (1970)], some 50 chemical elements have been identified, measured and classified according to size distribution type in such samples. For the purposes of cloud physics,and the evaluation of air cleansing by precipitation, among others, the problem remains to determine the exact molecular nature of the airborne particles. McCrone et al (1967) have given about 400 photomicrographs of various particles but nothing is yet reported about the formation and growth of crystalline particles during the sampling of aerosols.

The manufacturer's calibration for the Andersen sampler is given in Table 1. These calibration data are derived by means of

Table 1

Andersen Sampler: Particle Size Distribution

Stage	No. of Jets	*Radius of jet $x10^{-2}$cm	*Jet velocity cm/sec	*Range of[1] Particle radius given $x10^{-4}$ cm	Range of[2] Particle radius observed $x10^{-4}$ cm
1	400	5.91	107.9	$\leq$ 4.6	5 - 13.0
2	400	4.57	179.5	2.75 - 4.6	1.5 - 6.0
3	400	3.56	296.9	1.65 - 2.75	1.0 - 2.5
4	400	2.67	527.6	1.0 - 1.65	0.5 - 1.0
5	400	1.71	1277.7	0.5 - 1.0	0.5 - 1.0 (2.5 - 5.0)
6	400	1.27	2328.7	$\sim$ 0.5	0.25 - 0.5 (2.5 - 15)
7	216	1.27	4312.4	< 0.5	0.25 - 0.5 (4 - 20)

*The values are given by the manufacturer [Andersen samplers (1968)]

[1]For spherical particles of unit density or other particles of aerodynamically equivalent dimensions. The size limits indicate the approximate 50% cut off points.

[2]Values are computed from observation under optical microscope. Values in parenthesis for stages 5, 6, and 7 corresponds to crystalline particles.

laboratory tests using spherical particles of unit density and a controlled flow rate of 1 cubic foot per minute. In practice it is observed that the classification of airborne particles is less sharply defined because of variable shapes and densities of the particles, and frequently because of difficulty in maintaining the specified flow rate throughout the necessary sampling period.

2. Sampling

The Andersen sampler (model 0203) modified by the addition of a seventh impaction stage was used to collect and separate airborne particles according to their sizes. During sampling, the sampler was covered with an inverted petri dish to prevent rain water or snow from entering into the sampler. Most sampling was done on the roof of East Engineering building (about 60 feet above ground level).

Samples of aerosols have been collected by different investigators from this department, [Nifong (1970), Harrison (1970), Rahn (1971)] for 8 to 20 hours and, also up to 6 days or more time, for various methods of chemical analysis, which did not include inspection of samples under microscope. In our laboratory sample collections were made for varying periods of time from 16 to 120 hours. These samples were observed under a microscope and typical photomicrographs are shown in Figures 1-12. In broad terms, these figures show particles of decreasing size collected on the respective impaction plates of stages 1 to 6. However, some of the particles on the 5th, 6th, and 7th stages were found to be much larger than was expected (see Table 1).

3. Microscopic Observation of Particles

Stage 1: The particles appeared dark when observed under transmitted light; however they were found to be of different colors

Figure 1. Particles collected on stage 1, also showing plant pollens (spherical) at the center of photograph. (Approx. x 155).

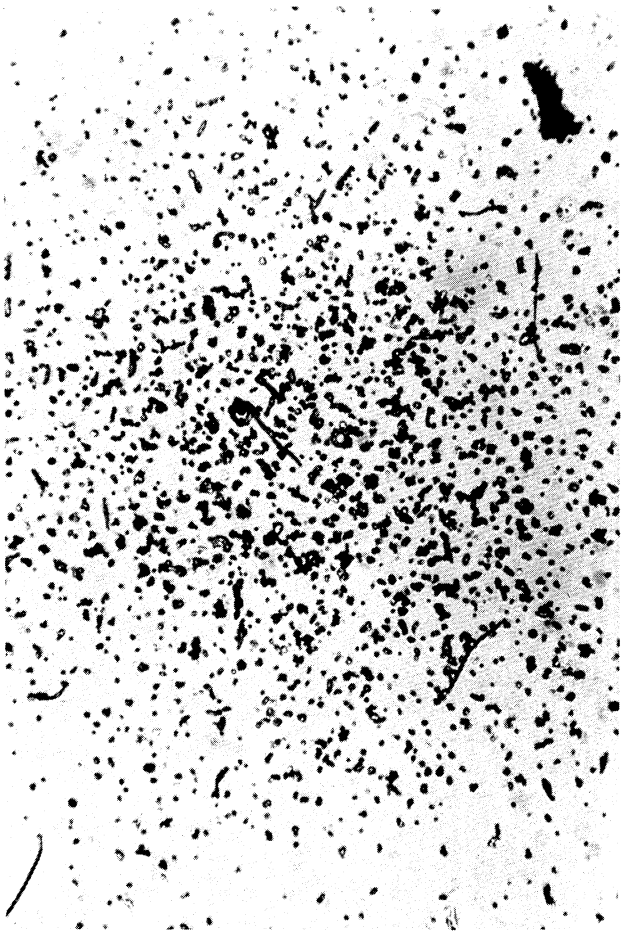

Figure 2. Particles collected on stage 2. Magnification as in Fig. 1.

Figure 3. Particles collected on stage 3. Magnification as in Fig. 1.

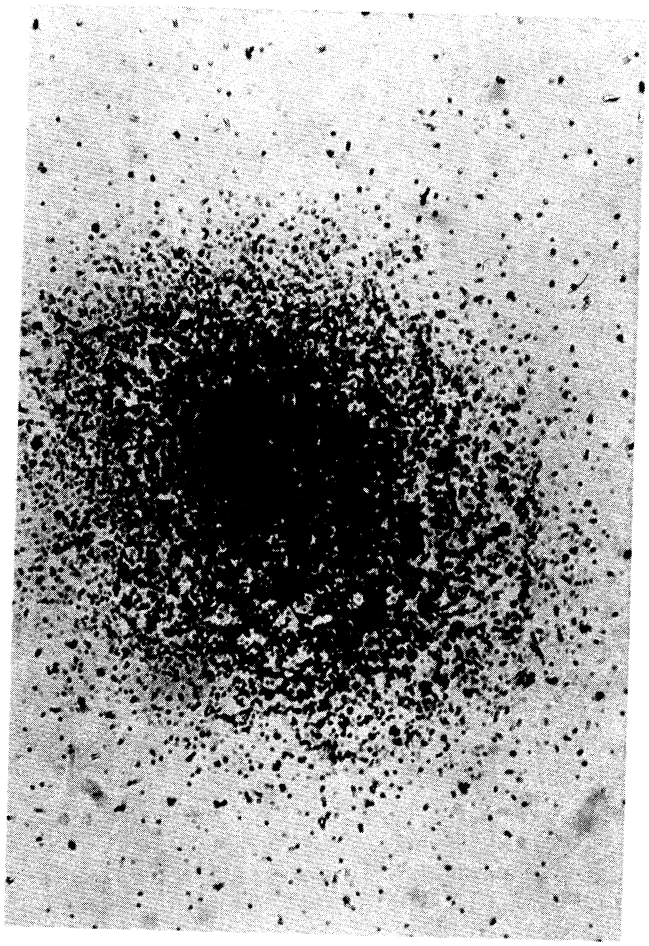

Figure 4. Particles collected on stage 4. Magnification as in Fig. 1.

Figure 5. Particles collected on stage 5 showing needle shaped crystalline particles. Magnification as in Fig. 1.

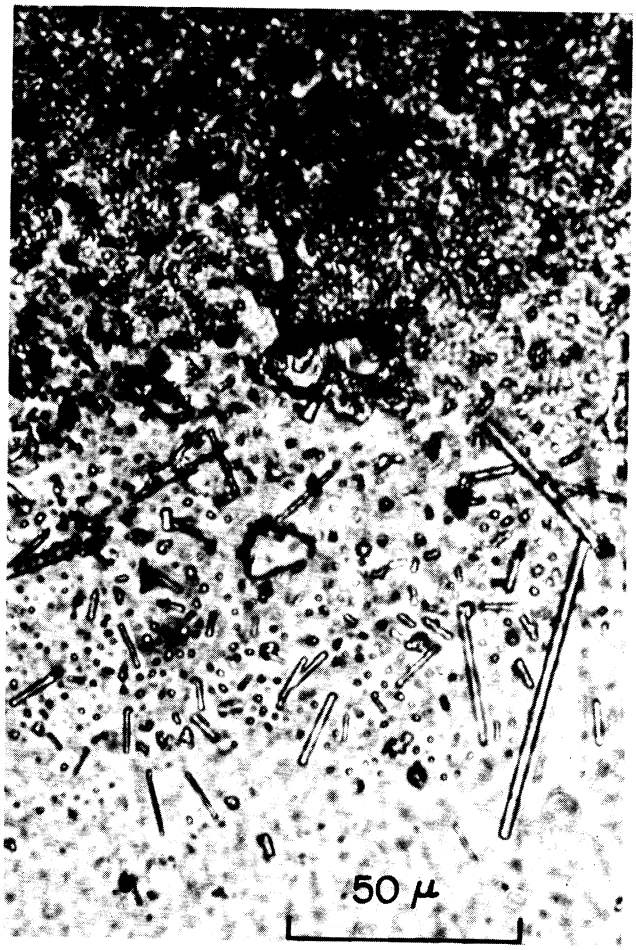

Figure 6. Stage 5. Magnification four times Fig. 1. (Approx. x 620).

Figure 7. Particles on stage 6. Magnification as in Fig. 1.

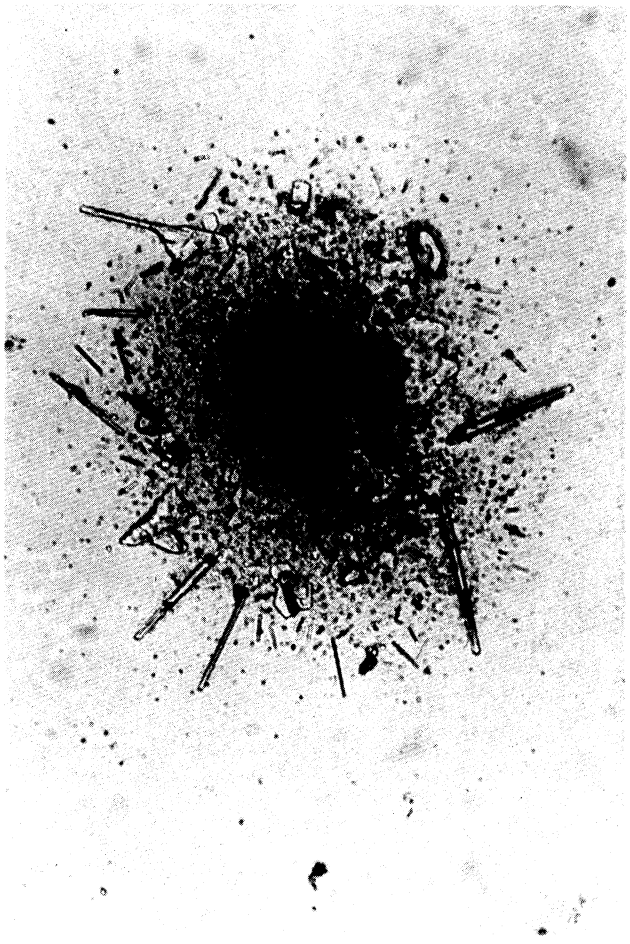

Figure 8. Typical needle shaped crystals including some irregular shapes on stage 7. Magnification as in Fig. 1.

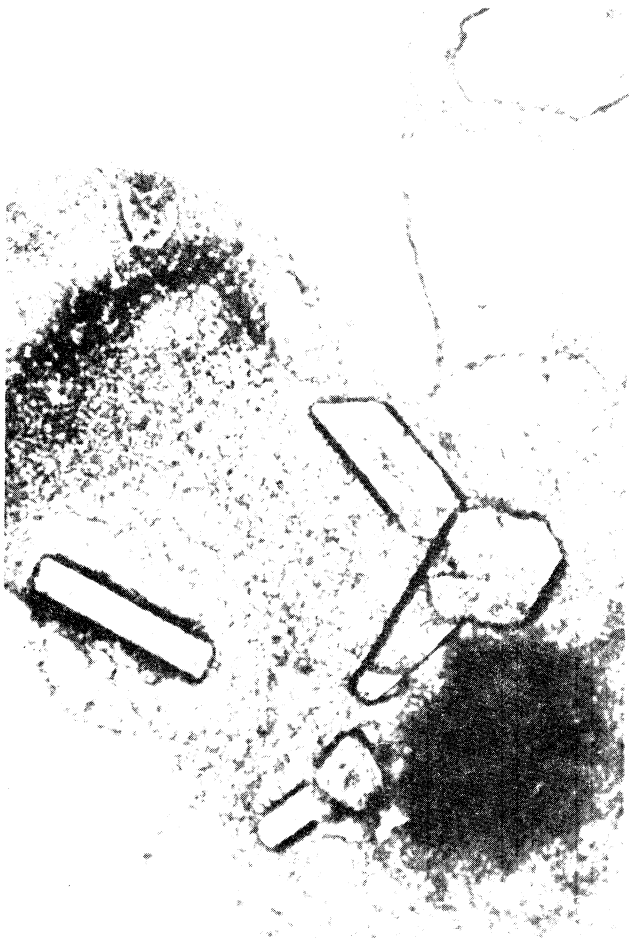

Figure 9. Large crystals growing in a droplet on stage 7. Magnification as in Fig. 1.

Figure 10. A single large crystal growing in a droplet on stage 7. Magnification as in Fig. 1.

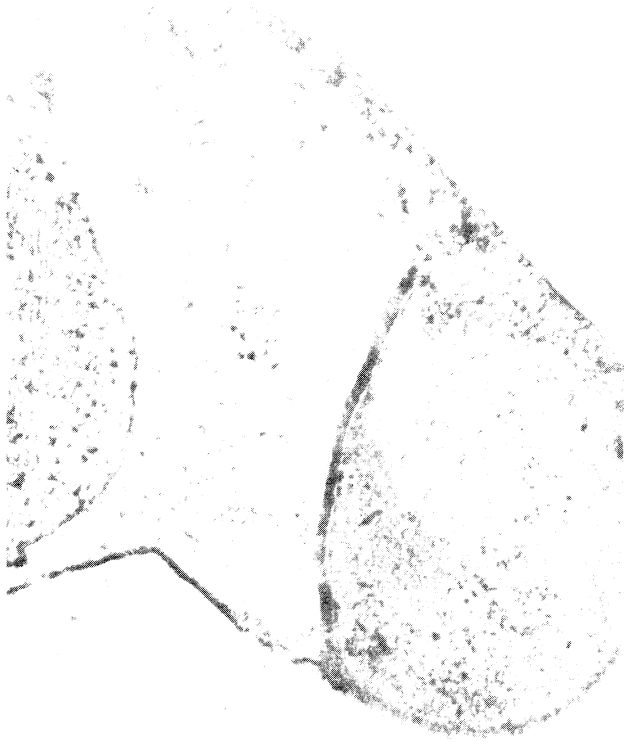

Figure 11. Photograph showing a droplet formed, when the sampling was stopped immediately after rain. Stage 7. Magnification as in Fig. 1.

Figure 12. Same droplet as in Fig. 11, photographs after 5 minutes showing recrystallization from the droplet. Magnification as in Fig. 1.

in reflected light, such as white, yellow, green, blue and rarely dark brown and red. They seem to be dust particles consisting mainly of silica. They were found to be insoluble in water and dilute (2N) HCl. The particles vary from 5 to 13 microns in radius, the average being about 7 microns. Some particles of flower pollen were also observed in this stage; they have a definite shape, whereas the other particles are of irregular shapes (Figure 1).

Stages 2 and 3: The particles collected on these impaction stages were found to be more or less identical in appearance to those of stage 1. They were slightly smaller in size and much greater in number, the latter being shown by their closeness on the sampling surface. The particle sizes of stage 2 range from about 1.5 - 6.0 microns in radius, the average being about 3.5 microns (Figure 2); those for stage 3 are from about 1.0 - 2.5 microns in radius with an average of about 2 microns (Figure 3).

The particles of stages 4 and 5 were found to be lying too close to each other to identify them as separate particles. It was difficult to resolve them and study their shape by an optical microscope (Figure 4,5). Under reflected light they appeared as an amorphous opaque mass. However in stage 5 some needle-shaped crystalline particles were found. Their width was about 1 to 2 microns while the length was from 6 to 15 microns (Figures 5,6). These particles were found to be readily soluble in water and insoluble in alcohol. [Note (Table 1) that the crystals tended to increase in size with increasing stage number].

In stage 6 (Figure 7) the particles were found to be partly (10 to 40 percent) crystalline and partly (60 to 90 percent) small

and opaque (carbon, silica, etc.).

The samples on stage 7 (Figure 8, 9, 10) were found to contain large crystals of various shapes; cubic, orthorhombic, acicular, and irregular. These were colorless and readily soluble in water and insoluble in alcohol. They were observed to increase in size as the sampling time was increased, and were frequently larger than the diameter of the air jet openings of this stage (25 microns). When, immediately after a rainfall the sampling was stopped and the sample sheet was observed under a microscope, we could observe a droplet slowly evaporating and small crystals appearing in that place. See Figures 11, 12.

4. X-Ray Crystallography

The crystalline particles from the samples (stage 6 and 7) were separated from the polyethylene film substrate and placed into a capillary tube for x-ray powder diffraction analysis. The quantity of sample was very small [~0.1mg] so that it could not be made into a fine powder; and hence the capillary was rotated during the experiment to obtain a uniform diffraction pattern of smooth lines rather than separate spots on the photographic film. Twenty-five significant diffraction lines were recorded out of which 22 lines agreed within 2% with the diffraction lines given for $(NH_4)_2SO_4$ [JCPDS (1972)]. Actually there are 30 diffraction lines for $(NH_4)SO_4$ between 5.31 Å and 1.945 Å, but 8 lines are of intensity $\leq$ 3% of the principal line and hence these 8 lines were not significantly noticed in the sample. The additional 3 lines observed in the diffraction pattern of the

sample were of about 35% intensity and could not be attributed to any reported compound. They may have arisen from some impurities carried with the crystalline particles during mechanical separation. The data of this experiment are given in table 2.

5. Chemical Analysis

The molecular composition of these crystalline particles was further confirmed by chemical analysis to be that of ammonium sulfate. For this experiment, the sampler was operated continuously for 50 hours, accumulating about 400 μgm of particles on stage 7. The crystals were separated from the sample by dissolving in distilled water. The solution was analyzed for NH_4^+ by colorimetry [Weatherburn (1967)] and for $SO_4^=$ by the barium chloranilate [Gales et al. (1968)] method. The ratio of amounts of NH_4 to SO_4 was found to be 0.38 which corresponds to the molecular formula $(NH_4)_2SO_4$. This ratio is equal to 0.2 for NH_4HSO_4 and 0.19 for $(NH_4)_2S_2O_8$.

To study the distribution of ammonium sulfate on each stage, a separate experiment was carried out. The sampler was operated continuously for 72 hours. A representative fraction from each stage was selected and the particles were dissolved in water and analyzed for $(NH_4)_2SO_4$ content. Table 3 shows the amount of $(NH_4)_2SO_4$ collected on each stage, and also the percentage of the total $(NH_4)_2SO_4$ collected on each stage during the experiment.

These data indicate that about 95% of the ammonium sulfate is collected on stages 5, 6 and 7. According to Table 1, particles normally collected on these stages are smaller than 0.5 micron in radius. It is not certain, because of the evident growth of $(NH_4)_2SO_4$ crystals, that the ammonium sulfate is deposited as

Table 2

X-ray Powder Diffraction Data

Line No.	Diffraction wavelengths in A° for $(NH_4)_2SO_4$ Powder*	Relative intensity with respect to principal line (4.33A°) I/I_1 in %	Diffraction wavelengths observed for sample in A°
1.	5.31	15	5.29
2.	5.22	30	5.19
3.	4.39	65	4.39
4.	4.33	100	4.33
5.	3.89	35	3.88
6.	3.66	<1	----
7.	----	--	----
8.	3.264	<1	----
9.	3.227	1	----
10.	3.139	30	3.139
11.	3.122	25	3.118
12.	3.055	55	3.048
13.	----	--	3.035
14.	----	--	3.006
15.	2.998	25	2.990
16.	2.839	1	----
17.	2.782	3	2.773
18.	2.704	5	2.705
19.	2.655	13	2.646

Table 2 (Cont.)

20.	2.611	7	2.604
21.	2.521	9	2.523
22.	2.476	3	----
23.	2.401	3	2.401
24.	2.374	3	----
25.	2.322	17	2.317
26.	2.317	20	2.317
27.	2.196	9	2.189
28.	2.168	15	2.168
29.	2.093	5	2.089
30.	2.062	<1	----
31.	2.005	<1	----
32.	1.973	5	1.973
33.	1.945	5	1.944
34.	1.942	5	1.944

*From JCPDS x-ray powder diffraction data file no. 10-343.

Note: Line numbers 6, 8, 9, 16, 22, 24, 30, and 31 of $I/I_1 \leq 3$ were too faint to observe in the sample spectrum.

Lines no. 7, 13, 14 from the sample spectrum could not be attributed to any known compound. Line no. 7 seems to correspond with the principal line of $PbSiO_3$ (3.34A°) however no other major lines of $PbSiO_3$ was observed.

Table 3

Ammonium Sulfate Collected on Various Stages Of Andersen Sampler

Stage No.	$(NH_4)_2SO_4$ in µgm	% of total $(NH_4)_2SO_4$ collected
1	10	<1
2	12	1
3	10	<1
4	30	2.6
5	270	23.
6	400	34.
7	450	38.

particles. However Heard and Wiffen (1969), report a maximum radius for ammonium sulfate particles to be 0.5 micron, determined by means of electron microscopy on millipore filter samples.

6. Results and Discussion

This finding (of table 3) above indicate that ammonium sulfate particles should have been collected mainly on stage 5, 6, and 7 of the Andersen sampler. The growth of large crystals may follow the small particle collection by other processes, e.g. solution and recrystallization. However two possible explanations can be put forward to the formation of these crystalline particles depending upon the microscopic observation and weather condition prevailing during sampling of aerosol.

1. Particles as seen on the photographs (Figure 5-8) were collected when the relative humidity was less than 40% during the sample collection, and the time of sample collection was between 20-40 hours. The particles were of fine needle-like shape and might have formed by the direct interaction of the constituents (NH_3, H_2O, SO_2, O_2) upon the surface of other smaller particles. The total mechanism of this reaction is very complex; but from the thermodynamic data, the reaction between these constituents to form $(NH_4)_2SO_4$ has a very large equilibrium constant $\sim 10^{47}$.

2. Crystalline particles as seen on the photographs (Figure 9-12) clearly appear to be forming from solution. This type of crystals was observed when there was relative humidity of 50% or more and possibly intermittent rain during the sampling time of

more than 20 hours.

When the incoming air is very humid and/or contains very fine droplets, the collected particles of the ammonium sulfate dissolve and form a solution in a droplet form on the sampling spot; later on relatively dry air passed through the sampler, dries the droplet by evaporation, and recrystallization into large crystals takes place. There is, in fact, a pressure drop of ∿65 millibars and a temperature rise of about 0.5° to 0.7°C from stage 1 to stage 7. This creates a favorable condition for evaporation of water from the later stages where it may be initially deposited in droplet form.

ACKNOWLEDGEMENTS

The authors wish to thank Professor J. D. Hanawalt of Materials and Metallurgical Engineering for his valuable assistance in interpretation of diffraction lines obtained in the x-ray crystallography experiment.

This research has been supported by the Earth Sciences Branch, Division of Biomedical and Environmental Research, U.S. Atomic Energy Commission, under Contract No.AT(11-1)-1407.

References

Andersen samplers (1968) Utah; now made by 2000 Inc., P.O. Box 7500, Utah.

Eggleton, A.E. J. (1969). The chemical composition of atmospheric aerosols on Tees-side and its relation to visibility. Atmos. Envir., 3, 355-372.

Gales, M. E. Jr., Kaylor, W. H., and Longbottom, J. E. (1968). Determination of sulfate by automatic colorimetric analysis. Analyst, 93, 97-100.

Garland, J. A., (1969). Condensation on ammonium sulfate particles and its effect on visibility. Atmos. Envir. 3, 347-354.

Harrison, P. R., (1970). Areawide distribution of lead, copper, cadmium and bismuth in atmospheric particles in Chicago and Northwest Indiana: a multi-sample application and anodic stripping voltammetry. University of Michigan Ph.D. thesis.

Healy, T. V., MacKay, H. A. C., Pilbeam A., and Scargill, D. (1970). Ammonia and ammonium sulfate in the troposphere over the United Kingdom. J. Geophys. Res., 75, 2317-2321.

Heard, M. J., and Wiffen, R. D. (1969). Electron microscopy of natural aerosols and the identification of particulate ammonium sulfate. Atmos. Envir., 3, 337-340.

Joint Committee on Powder Diffraction Standards (1972). Index to the powder diffraction file. Prepared and published by JCPDS, 1601 Parklane, Swarthmore, Pennsylvania.

Junge, C. (1954). The chemical composition of atmospheric aerosols. 1: measurement at Round Hill field station June-July, 1953. J. Met. 11, 323-333.

Junge, C. E. and Ryan, T. G. (1958). Study of the SO_2 oxidation in solution and its role in atmospheric chemistry. Quart.J. Roy. Met. Soc. 84, 46-55.

McCrone, W. C., Draftz, R. G. and Delly, J. G. (1967). The particle atlas. Ann Arbor Science Publishers, Inc., Ann Arbor, Michigan.

Nifong, G. D. (1970). Particle size distribution of trace elements in pollution aerosols. University of Michigan Ph. D. thesis.

Rahn, K. A. (1971). Sources of trace elements in aerosols. An approach to clean air. University of Michigan Ph.D. thesis.

Weatherburn, M. W. (1967). Phenol-hypochlorite reaction for determination of ammonia. Anal. Chem. 39, 971-974.

Van den Heuvel, A. P. and Mason, B. J. (1963). The formation of ammonium sulfate in water droplets exposed to gaseous sulfur dioxide and ammonia. Quart. J. Roy. Met. Soc. 89, 271-275.

SECTION IV. ADMINISTRATIVE

A. PUBLICATIONS

COO-1407-39 Rain Scavenging Studies, by A.N. Dingle, Progress Report No. 8, Contract No. AT(11-1)1407, U.S. Atomic Energy Commission, Dept. of Meteorology and Oseanography, The University of Michigan, Ann Arbor. January 1972. 103 + v.pp.

COO-1407-40 "Man-made climatic changes: seeding by contrails" by A. N. Dingle, Science, 173, 461, 30 July 1971.

COO-1407-41 "Terminal fallspeeds of raindrops" by A.N. Dingle and Y. Lee. J. Applied Meteor., 11, 877-9, Aug. 1972.

COO-1407-42 Abstract of "Transport and deposition of tracer indium in a frontal convective shower situation" by A. N. Dingle. Bul.Amer.Meteorol.Soc.,53, 1058, Oct., 1972.

COO-1407-43 Abstract of "A scavenging model for steady rain" by A.N. Dingle and Y. Lee. Bul.Amer.Meteor.Soc.,53, 1065, Oct., 1972.

COO-1407-44 Abstract of "Nucleation, growth, and removal by rain of haze and fog in a stratum of polluted air" by P. B. Storebø and A.N. Dingle. Bul.Amer.Meteorol. Soc., 53, 1065, Oct., 1972.

COO-1407-45 "Removal of pollution by rain in a shallow air flow" by P. B. Storebø and A. N. Dingle. Submitted to J. Atmos. Sci., April, 1973.

COO-1407-46 "An analysis of in-cloud scavenging" by A. N. Dingle and Y. Lee. Submitted to J. Applied Meteor., May, 1973.

COO-1407-47 "Ammonium sulfate crystallization in Andersen cascade impactor samples" by A. N. Dingle and B. M.Joshi. Submitted to Atmospheric Environment, June, 1973.

COO-1407-48 Abstract of "Removal of pyrotechnic generated tracer placed by aircraft in a convective updraft" by A.N. Dingle. Submitted April, 1973 to WMO/IAMAP International Conference on Weather Modification, 1-7 October, 1973, Tashkent, USSR. Accepted for presentation 15 June 1973.

B. PERSONNEL

1. Mr. Yean Lee, Ph.D. Candidate, research associate

2. Mr. Duane Harding, Ph.D. Candidate, research associate

3. Mr. B. M. Joshi, analytical chemist, graduate student with Departments of Chemistry and Atmospheric and Oceanic Science jointly, research assistant

4. Mr. Nolan Doesken, part time student assistant